Forum for Electromagnetic Research Methods and Application Technologies (FERMAT)

# Ground plane assisted Miniaturization of Multiband and Wideband printed Monopole Antennas

Thesis Defense Seminar

Prashant Garg

Supervisor: Prof. Tarun Kanti Bhattacharyya

Advanced Technology Development Center

Indian Institute of Technology Kharagpur

May 2016

# Abstract

In the presented research, various aspects of miniaturization have been investigated to design compact antenna solutions for specific operating environments, and a better understanding of design optimization and their prospects developed. For multiband operation in the low and mid-frequency spectrum covering LTE and other protocols, ground plane curvature is utilized to achieve lowering of the narrowband frequency to 630 MHz in the proposed annular split ring monopole antenna. Its wideband impedance match characteristics (2 - 4.23 GHz) are seen to remain relatively unaffected by variation of band-rejection locations over its bandwidth. Despite being designed in low permittivity, thin substrate ($\varepsilon_r$ = 2.2, 1/16th inch), at 48 × 44 $mm^2$ , the antenna has the most compact size reported so far for the narrowband coverage provided. For wideband coverage of nearly all FDD and TDD LTE bands, ground plane based feed gap variations have been found critical in obtaining the ultra-wide bandwidth (0.7 – 3.4 GHz) and securing stability in its lower and upper edge cut-off frequencies. Constructed in 'long-board' configuration with dimensions of 105 × 40 $mm^2$ on $1/16^{th}$ inch thick FR4 laminate ($\varepsilon_r$ = 4.4), its higher radiation resistance maintains higher cross-polar levels and efficiency throughout its bandwidth.

A systematic design approach harnessing miniaturization potential of stepped impedance resonator theory is applied to the development of a dual-resonant high frequency wideband antenna, where transmission line modelling has been found to hold well beyond ground plane edges. Further, fine tuning of impedance match characteristics between resonances by ground plane based stubs were found to reduce reflection and render the compact antenna (35 × 30 $mm^2$ , $\varepsilon_r$ = 2.2) operational over nearly an ultrawide bandwidth (3.2 – 11 GHz), which nearly covers the entire FCC UWB spectrum.

Finally, a more comprehensive take towards miniaturization is offered through a topology alteration that seeks to improve both miniaturization and radiation performance of antennas. The 'stripline-fed superstrate' topology, results in a 'sandwich' type structure of the antenna with a stripline feed. An 11% downshift in dominant resonance frequency for a strip monopole as compared to its microstrip counterpart, and higher cross polar levels are seen resulting from better dielectric homogenization and superstrate cover effects that the topology provides. Further, width-wise direct downscaling of the previously discussed low frequency rectangular disc wideband antenna to this topology has found it retaining its original wideband and radiation characteristics, but with a 37.5 % reduction in surface area. This observed direct adaptation of existing designs seems to hold future promises of its wider application. The work in this presentation may thus help antenna designers expand their scope of options, or perspective of approach, for confronting miniaturization issues of printed monopole antennas.

**Index terms:** monopole antennas, miniaturization, ground-plane based, low frequency, LTE, bandwidth enhancement, multiband, wideband, ultra wideband, tunable band-rejection, transmission line theory, stepped impedance resonator, design topology, stripline-fed superstrate

# Biography

**Prashant Garg** (S'08–M'17) received his B.Tech degree in electronics and communication engineering and M. Tech degree in automation and computer vision from Indian Institute of Technology, Kharagpur, India in 2005 and 2006, respectively. He received the M. Eng. degree in electrical engineering from Rensselaer Polytechnic Institute, Troy, NY, USA in 2010, and Ph.D. degree from IIT Kharagpur, India in 2016.

From 2006 to 2010, as a researcher at RPI, Troy, NY., he helped develop a microwave based thermocycler prototype for highly energy efficient RNA RT-PCR reactions. His Ph. D. work has demonstrated significant miniaturization potential of tailoring ground planes in producing wideband and multiband LTE domain planar antennas. A new topology of ground-plane based design offering even further miniaturization for planar antennas was introduced and filed for patent. He has held teaching positions in India at National Institute of Technology (NIT), Hamirpur, NIT Delhi, Netaji Subhash University of Technology, Delhi and Delhi University, South Campus.

# Contents

# Antenna Miniaturization

- Fast changes in wireless communication have shrunk size and reduced weight of handheld terminal devices.
- A higher level of integration of dis-similar components at the chip or board level is expected.
- While communication bands stay in the lower frequency range, antenna dimensions have not been able to scale proportionately with chip size.

→ Antenna Miniaturization

Light weight Flexible Planar Monopole Antenna[b]

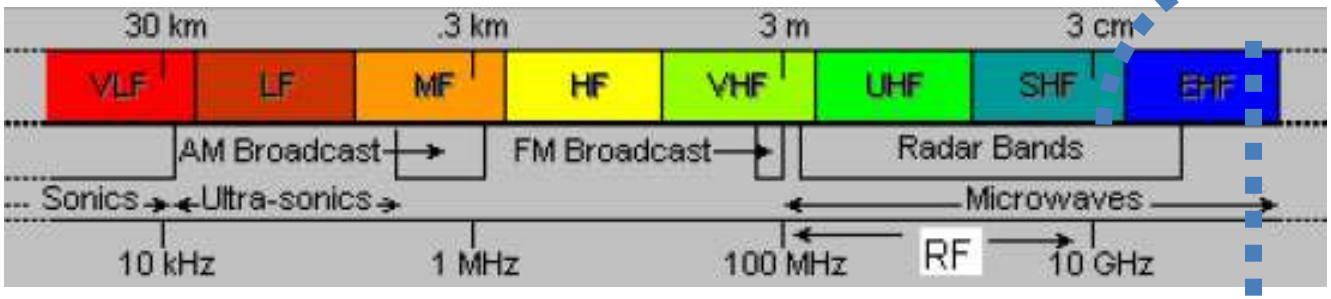


EM spectrum[a]

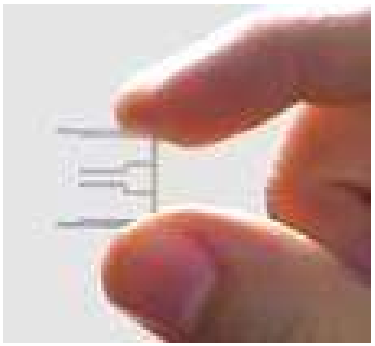

Miniaturized TV Antenna[c]

[a] http://sss-mag.com/spectrum.html
[b] Image sourced from: http://www.intechopen.com/source/html/37715/media/image1.png
[c] http://www.offthereservation.net/2013/04/aereo-future-of-television.html

# Motivation

Meandering

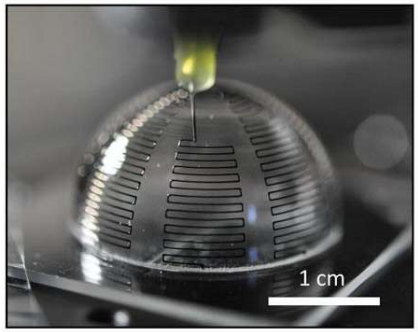


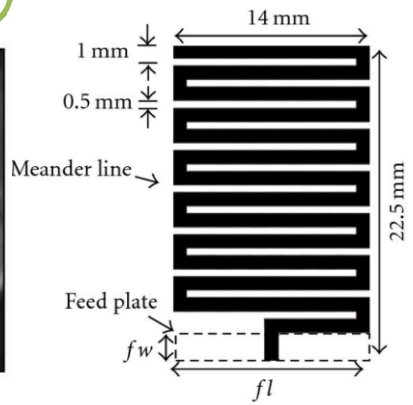


Meandering of the radiator in a planar printed Antenna[e]

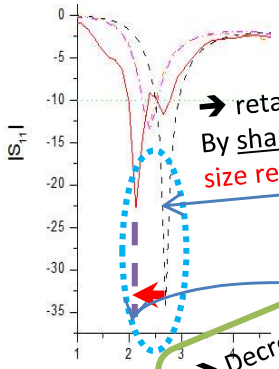


➔ retain original resonance By shape modification, after Antenna size reduction, e.g. meandering

➔ Decreasing dominant resonance By permittivity up-scaling or shape modification ; Antenna size = constant

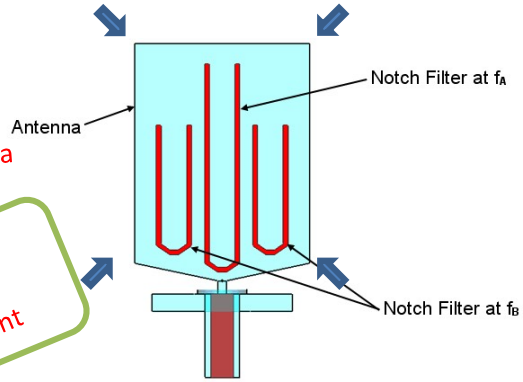


Monopole Antenna[d]

Impedance Bandwidth

Size Reduction

Antenna Miniaturization: Target

Radiator length change required is significant for even small decrease in resonance frequency.

Radiation Pattern

Gain & Efficiency

$\ell \alpha 1/v$

$\ell$: resonant length of antenna

v: target resonance frequency

! Problem for low frequency design:

Approaches ?

Shape

Configuration

Topology

Objective: To research miniaturization techniques for multiband and wideband antennas in the low and mid-frequency (sub-GHz and GHz) domain.

[d] Image source: https://www.cst.com/Content/Articles/article271/Monopole%20Antenna%20with%20Notch%20Filter%20Components.gif

[e] Image source: http://www.nanotech-now.com/news_images/42004.jpg

| FDD LTE BANDS & FREQUENCIES | | | | | |
|---|---|---|---|---|---|
| LTE BAND NUMBER | UPLINK (MHZ) | DOWNLINK (MHZ) | WIDTH OF BAND (MHZ) | DUPLEX SPACING (MHZ) | BAND GAP (MHZ) |
| 1 | 1920 - 1980 | 2110 - 2170 | 60 | 190 | 130 |
| 2 | 1850 - 1910 | 1930 - 1990 | 60 | 80 | 20 |
| 3 | 1710 - 1785 | 1805 -1880 | 75 | 95 | 20 |
| 4 | 1710 - 1755 | 2110 - 2155 | 45 | 400 | 355 |
| 5 | 824 - 849 | 869 - 894 | 25 | 45 | 20 |
| 6 | 830 - 840 | 875 - 885 | 10 | 35 | 25 |
| 7 | 2500 - 2570 | 2620 - 2690 | 70 | 120 | 50 |
| 8 | 880 - 915 | 925 - 960 | 35 | 45 | 10 |
| 9 | 1749.9 - 1784.9 | 1844.9 - 1879.9 | 35 | 95 | 60 |
| 10 | 1710 - 1770 | 2110 - 2170 | 60 | 400 | 340 |
| 11 | 1427.9 - 1452.9 | 1475.9 - 1500.9 | 20 | 48 | 28 |
| 12 | 698 - 716 | 728 - 746 | 18 | 30 | 12 |
| 13 | 777 - 787 | 746 - 756 | 10 | -31 | 41 |
| 14 | 788 - 798 | 758 - 768 | 10 | -30 | 40 |
| 15 | 1900 - 1920 | 2600 - 2620 | 20 | 700 | 680 |
| 16 | 2010 - 2025 | 2585 - 2600 | 15 | 575 | 560 |
| 17 | 704 - 716 | 734 - 746 | 12 | 30 | 18 |
| 18 | 815 - 830 | 860 - 875 | 15 | 45 | 30 |
| 19 | 830 - 845 | 875 - 890 | 15 | 45 | 30 |
| 20 | 832 - 862 | 791 - 821 | 30 | -41 | 71 |
| 21 | 1447.9 - 1462.9 | 1495.5 - 1510.9 | 15 | 48 | 33 |
| 22 | 3410 - 3500 | 3510 - 3600 | 90 | 100 | 10 |
| 23 | 2000 - 2020 | 2180 - 2200 | 20 | 180 | 160 |
| 24 | 1625.5 - 1660.5 | 1525 - 1559 | 34 | -101.5 | 135.5 |
| 25 | 1850 - 1915 | 1930 - 1995 | 65 | 80 | 15 |
| 26 | 814 - 849 | 859 - 894 | 30 / 40 | | 10 |
| 27 | 807 - 824 | 852 - 869 | 17 | 45 | 28 |
| 28 | 703 - 748 | 758 - 803 | 45 | 55 | 10 |
| 29 | n/a | 717 - 728 | 11 | | |
| 30 | 2305 - 2315 | 2350 - 2360 | 10 | 45 | 35 |
| 31 | 452.5 - 457.5 | 462.5 - 467.5 | 5 | 10 | 5 |

| TDD LTE BANDS & FREQUENCIES | | |
|---|---|---|
| LTE BAND NUMBER | ALLOCATION (MHZ) | WIDTH OF BAND (MHZ) |
| 33 | 1900 - 1920 | 20 |
| 34 | 2010 - 2025 | 15 |
| 35 | 1850 - 1910 | 60 |
| 36 | 1930 - 1990 | 60 |
| 37 | 1910 - 1930 | 20 |
| 38 | 2570 - 2620 | 50 |
| 39 | 1880 - 1920 | 40 |
| 40 | 2300 - 2400 | 100 |
| 41 | 2496 - 2690 | 194 |
| 42 | 3400 - 3600 | 200 |
| 43 | 3600 - 3800 | 200 |
| 44 | 703 - 803 | 100 |

# Literature Review

## Multibranch IFA antenna[1]

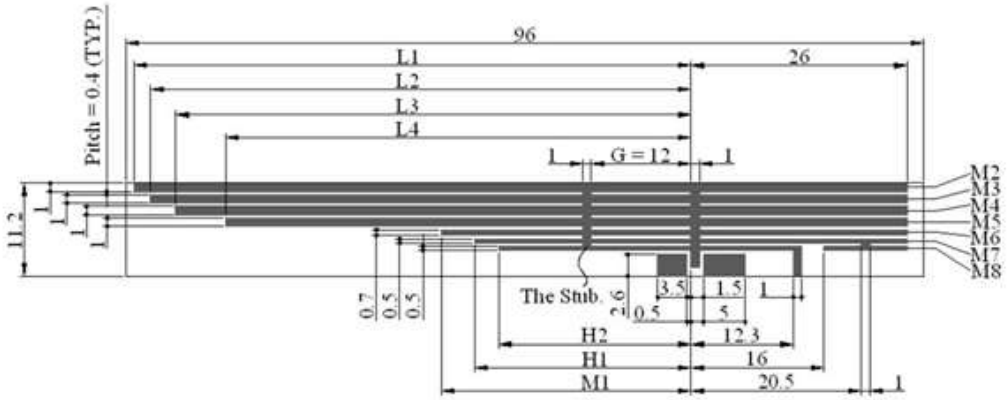


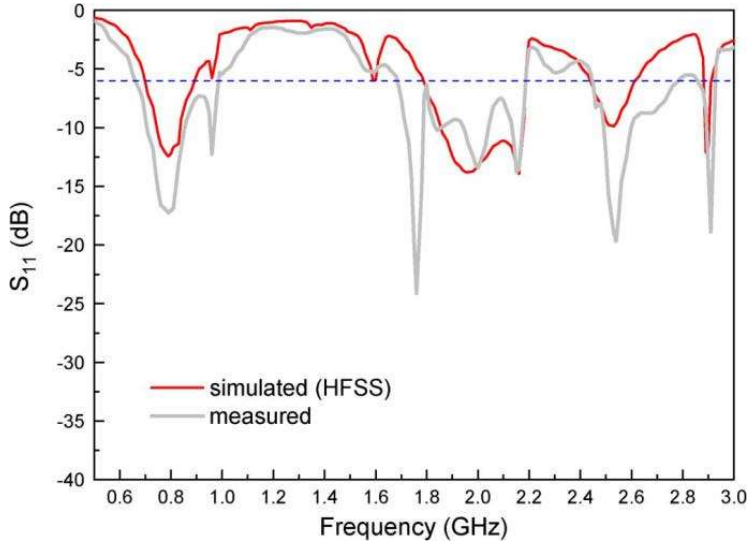


Uses multi-branch resonant strips and intermediate coupling pads: dimensions of 96 x 11.2 mm$^2$

Min. resonance band: 663 – 993 MHz

## Inductively coupled PIFA antenna[2]

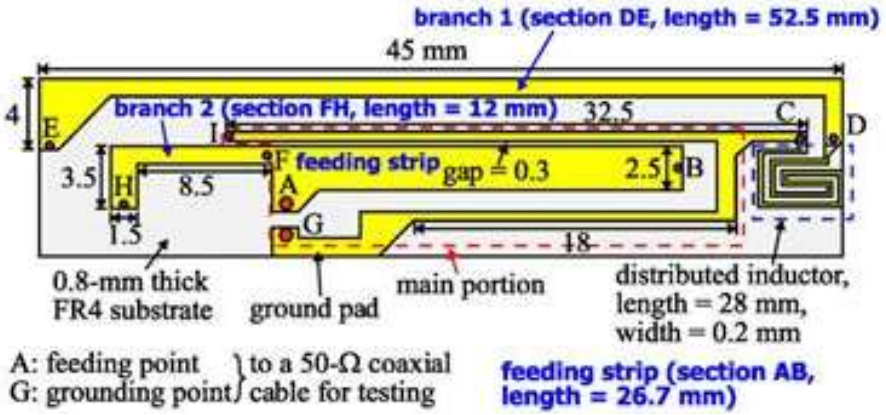


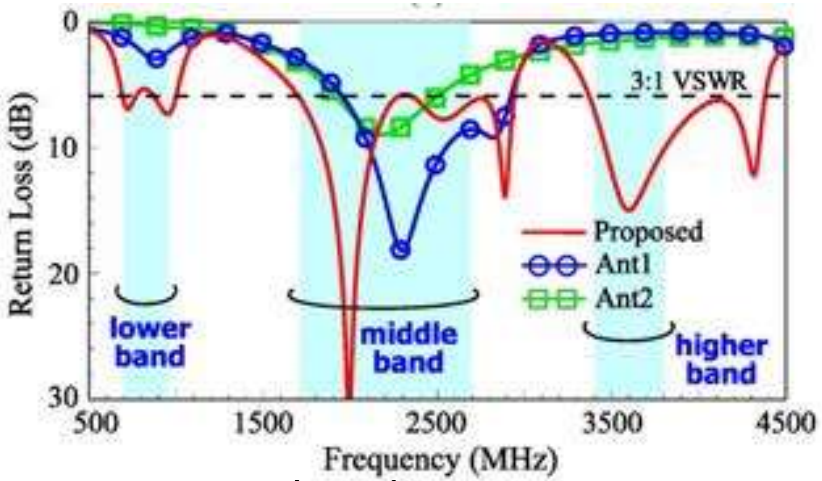


Inductively coupled branch strip: 45 x 10 mm$^2$

Min. resonance band: 698 – 960 MHz

2. Multiband LTE Antenna Design and Optimization

# Literature Review

## Monopole with Archemedian Spiral[4]

Variable length spiral creates multiband response: 35 x 35 mm$^2$

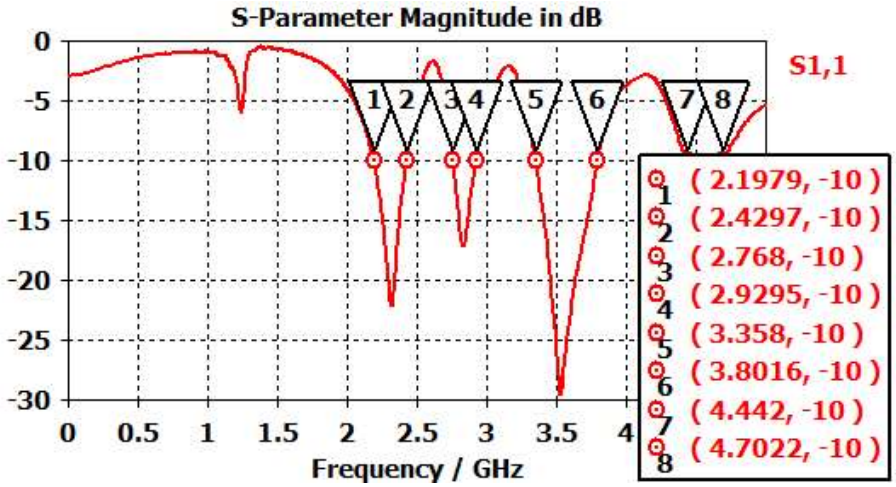


Min. resonance band: 2190 – 2430 MHz

## Inkjet printed Concentric Monopole[5]

Variable length concentric radiator steps spiral with curved ground plane: 70 x 70 mm$^2$

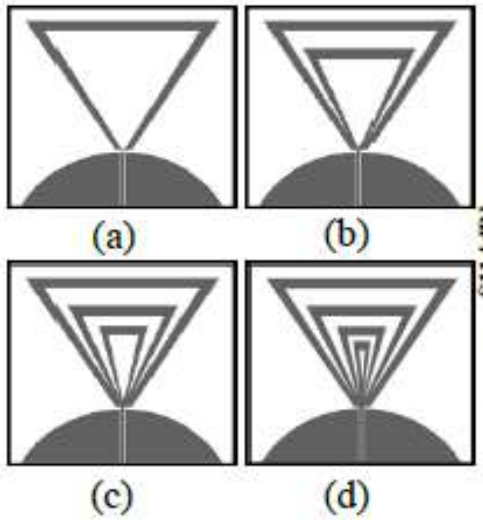


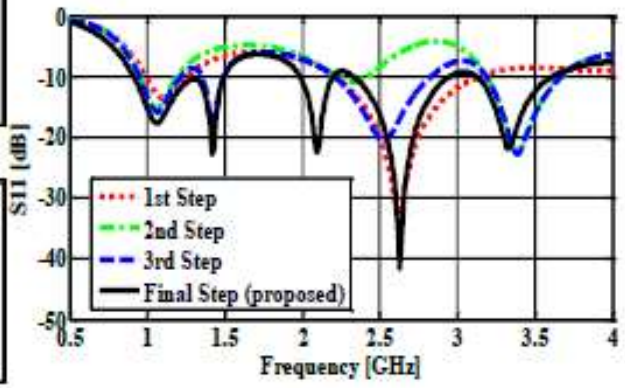


Min. resonance band: 870 – 1520 MHz

# 2. Annular Split-Ring Multiband Antenna

Objective

To achieve reduction in lowest frequency of operation (targeting low frequency LTE band) , but with minimum area requirement and with low permittivity substrate

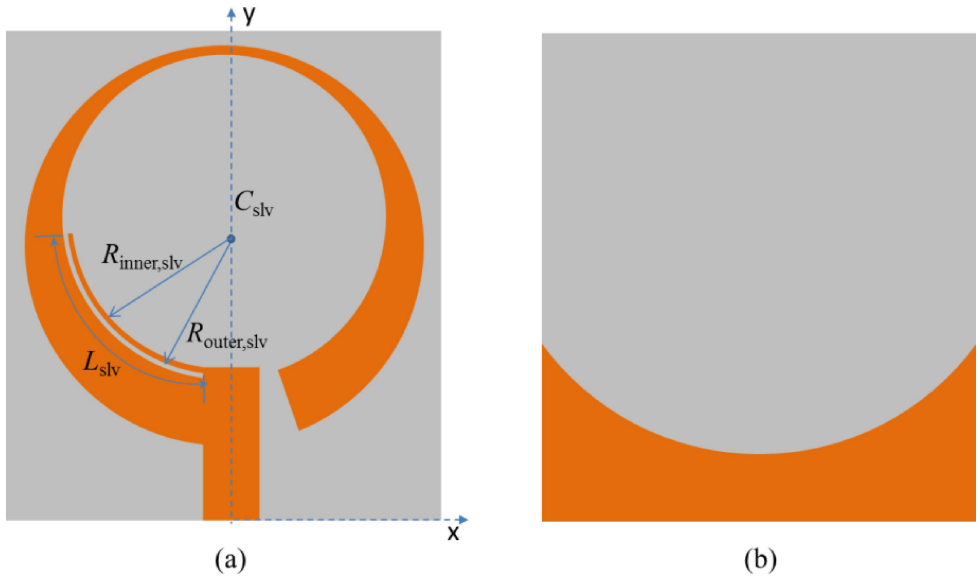


(a) Top view and (b) Rear View of the Multiband antenna

## 2.1 Initial Design

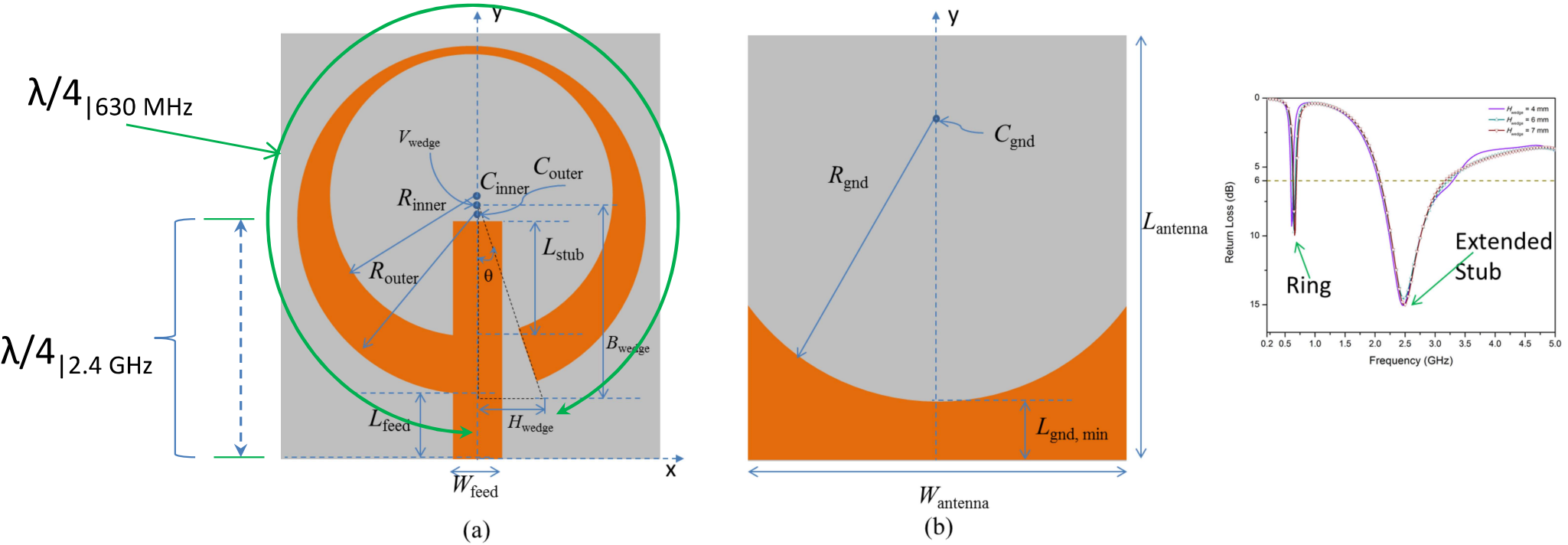


Initial design was planned as a dual resonant antenna with the ring providing for the first resonance (132 mm) and the extended stub *i.e. Feed + ring cross-section + stub length* (27 mm) contributing towards the second resonance.

Table 1. Values of design parameters for the multiband antenna

| Parameter | $L_{feed}$ | $L_{antenna}$ | $L_{gnd,min}$ | $L_{stub}$ | $B_{wedge}$ | $H_{wedge}$ | $V_{wedge}$ |
|---|---|---|---|---|---|---|---|
| Values (mm) | 7 | 48 | 6 | 13.5 | 21.5 | 4 | (0, 27.5) |
| Parameter | $W_{feed}$ | $W_{antenna}$ | $C_{inner}$ | $C_{outer}$ | $R_{inner}$ | $R_{outer}$ | $C_{gnd}$ |
| Values (mm) | 4.7 | 44 | (0,30) | (0,27) | 16 | 20 | (0,40) |
| Parameter | $R_{gnd}$ | $C_{slv}$ | $R_{inner, slv}$ | $R_{outer, slv}$ | $L_{slv}$ | | |
| Values (mm) | 34 | (0,30) | 15 | 15.7 | 26 | | |

## 2.2 Parametric Simulations and Design modification


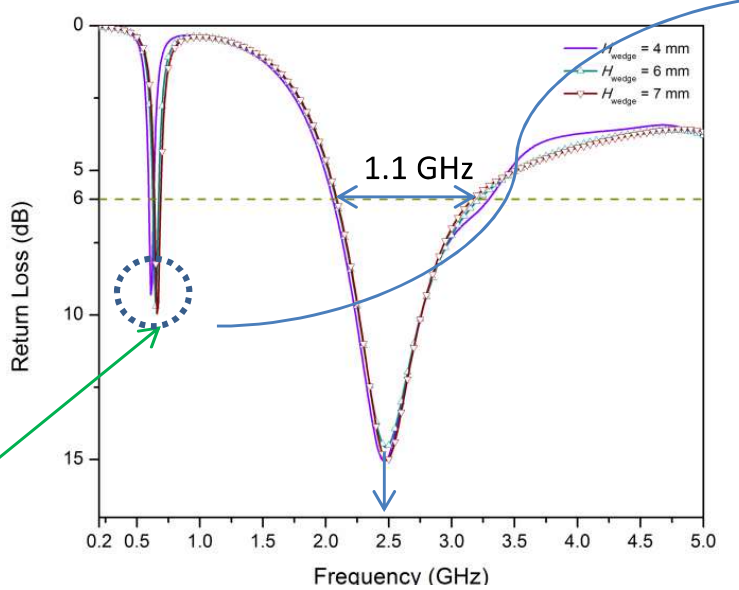


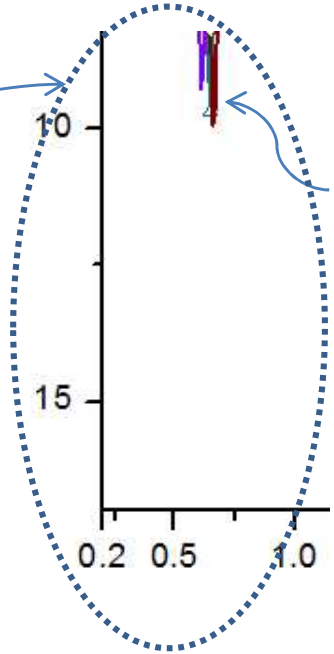


610 to 660 MHz variation due to ring length

Upper resonance stays nearly constant about 2.48 GHz

Wedge height variation

Stub length variation

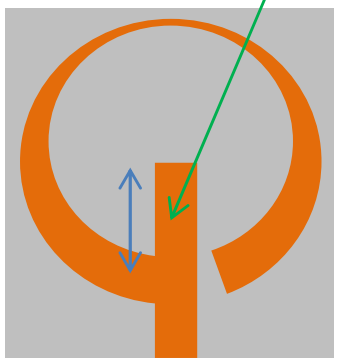

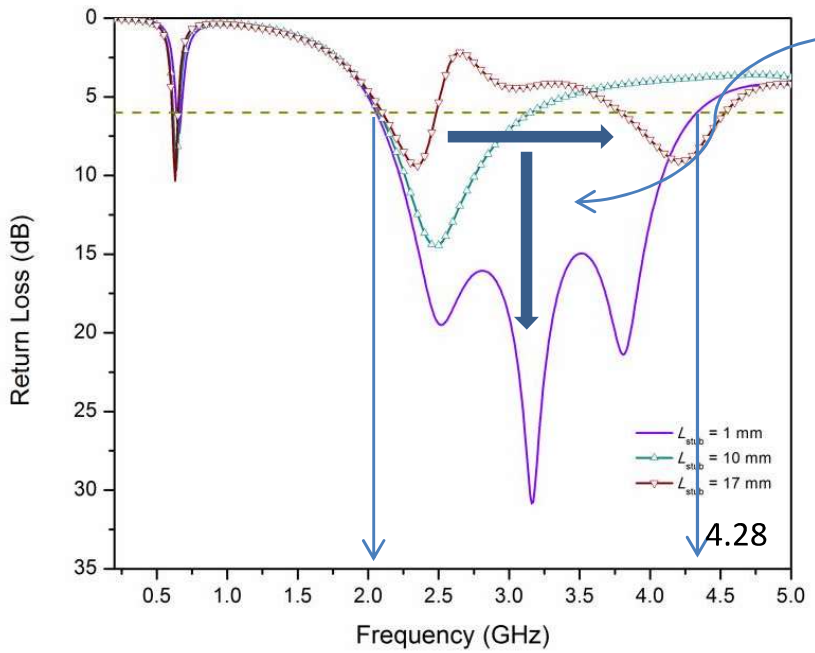


Reduced inductive effect improves impedance match

Motivation to remove stub

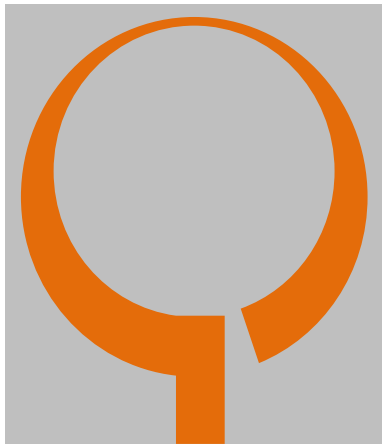

## 2.2 Parametric Simulations and Design modification

### Annular Cross-section variation

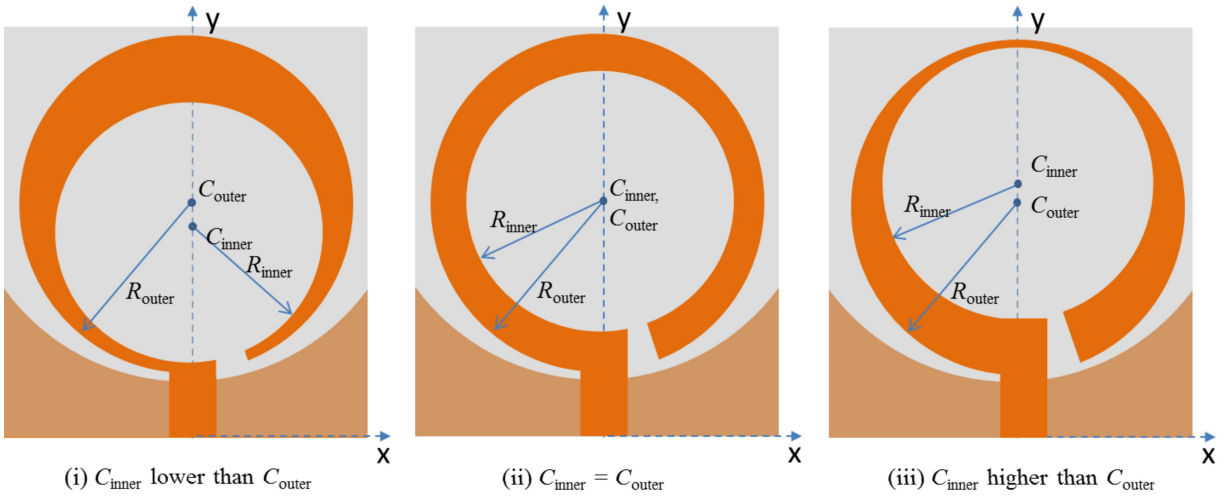


(i) $C_{inner}$ lower than $C_{outer}$ (ii) $C_{inner}$ = $C_{outer}$ (iii) $C_{inner}$ higher than $C_{outer}$

Due to reduced capacitance resulting from separation of wider arc away from ground

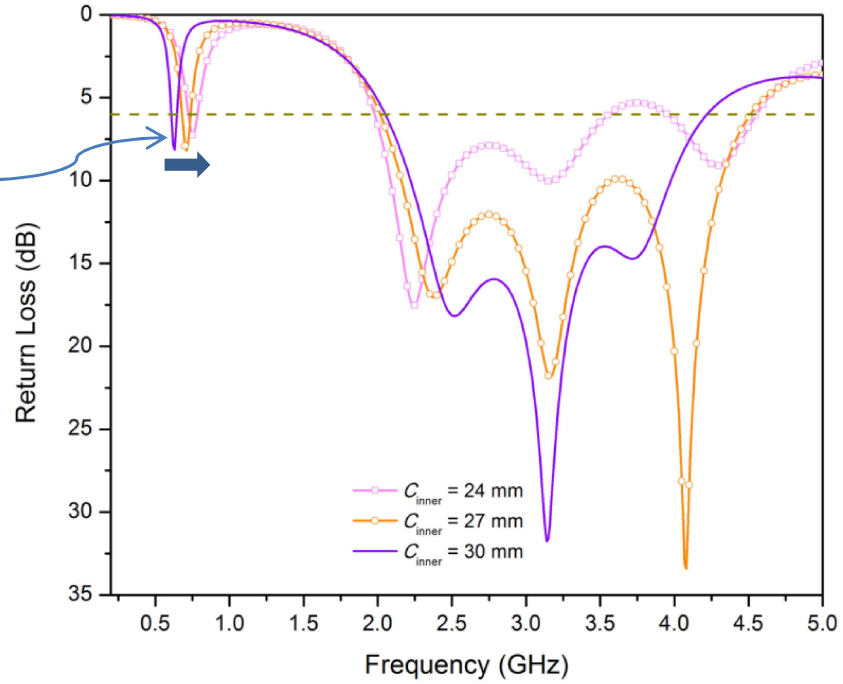


Preference for (iii) due to smaller value of narrowband resonance

## 2.2 Parametric Simulations and Design modification

### Band Reject functionality – Sleeve based

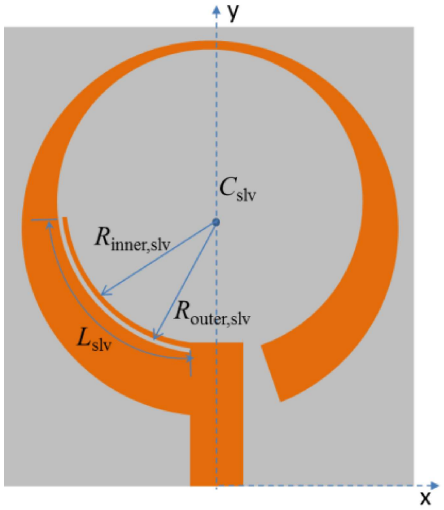


A curved sleeve is used for achieving intermediate band rejections in order to filter out undesired signal frequencies.

The variations in sleeve length can be explained as an open-circuited stub attached in parallel to the radiator.

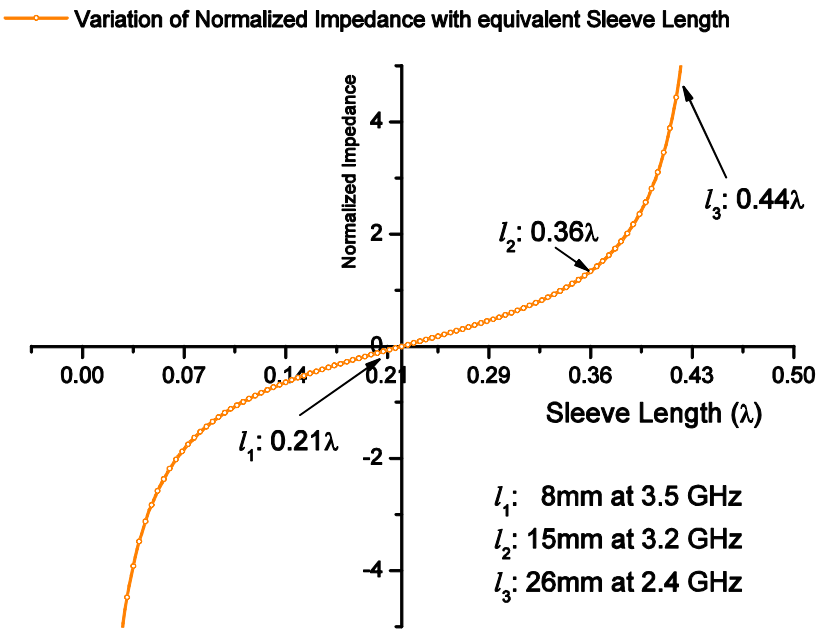


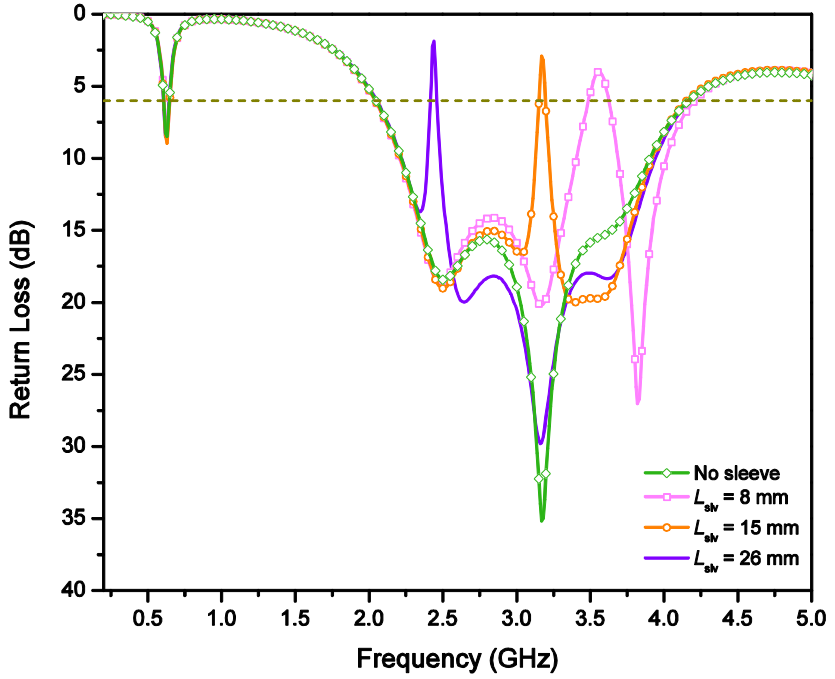

## 2.2 Parametric Simulations and Design modification

### Effect of ground plane curvature

A convex shaped plane having a similar radius of curvature (as of a concave ground, R = 34 mm) was simulated. It shows a general upward shift of the dominant and subsequent resonance frequencies along with their respective bands. This is due to reduced gap capacitances following an increase in separation between the radiator and ground plane.

This upward shift in resonances is also noticed for the uniform ground plane, but is more pronounced for a convex ground plane structure.

Yes, the convex ground plane provides a wider impedance match of 4 GHz (2.23 – 6.23 GHz), but has the lower edge frequency shifted upwards to 2.23 GHz. The band-rejection frequency is seen to stay same as that of the uniform ground plane, at 2.68 GHz, and the lowest resonance frequency increases to 700 MHz.

Convex Ground (R = 34 mm)

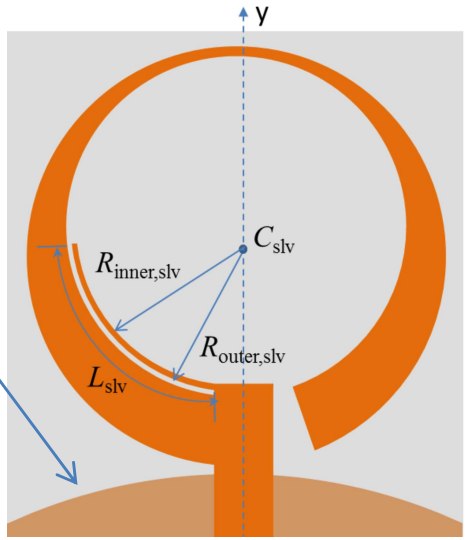


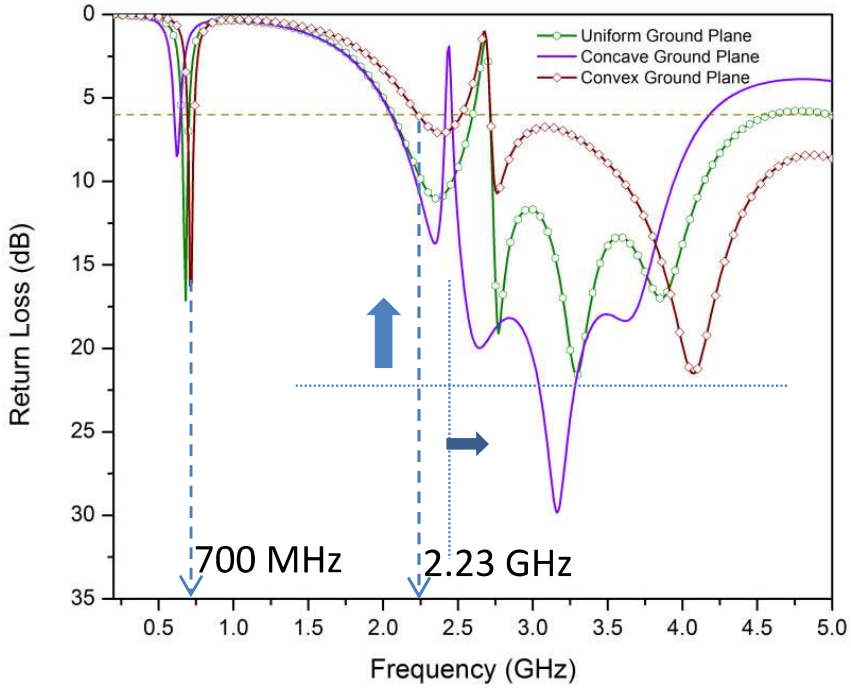

## 2.3 Measurement Results

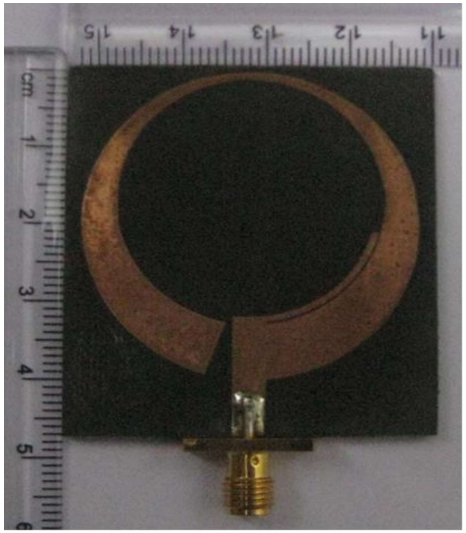

(a)

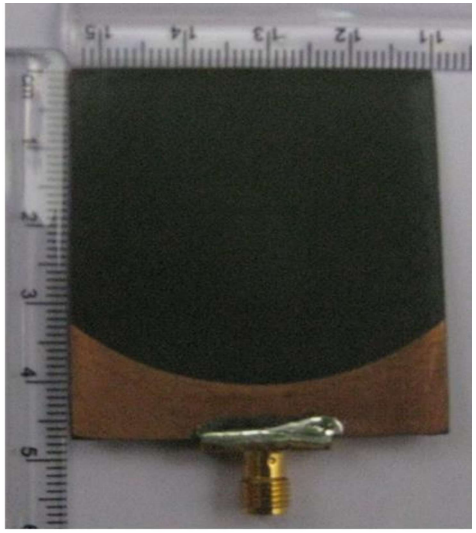

(b)

(a) Top and (b) Rear View of fabricated antenna

The annular split ring multiband antenna prototype is fabricated fabricated on a 1/16" (1.5875 mm) thick Rogers 5008 board ($\varepsilon_r$ = 2.2) of dimensions 48 × 44 $mm^2$.

Design dimensions are as illustrated earlier in Table 1.

### Return Loss measurements

Measured narrowband match is deeper and shows an increased bandwidth of 65 MHz about 630 MHz.

An overall gradual shift of impedance match characteristics towards higher frequencies.

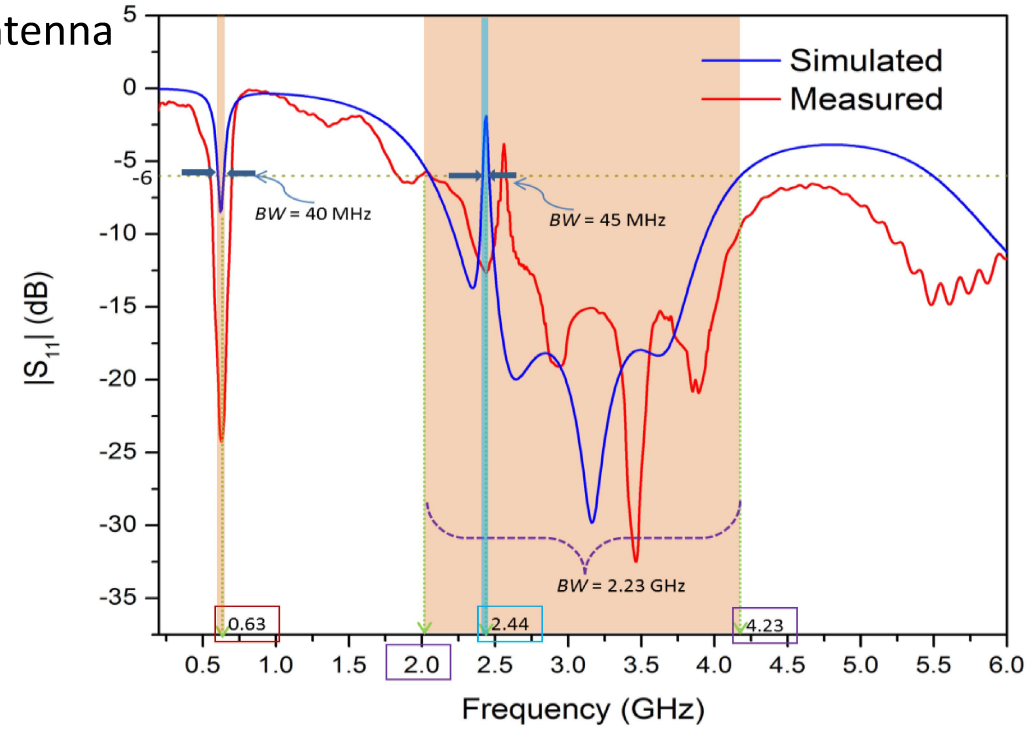

## 2.3 Measurement Results

### Radiation Pattern at narrowband resonance (630 MHz)

E - plane

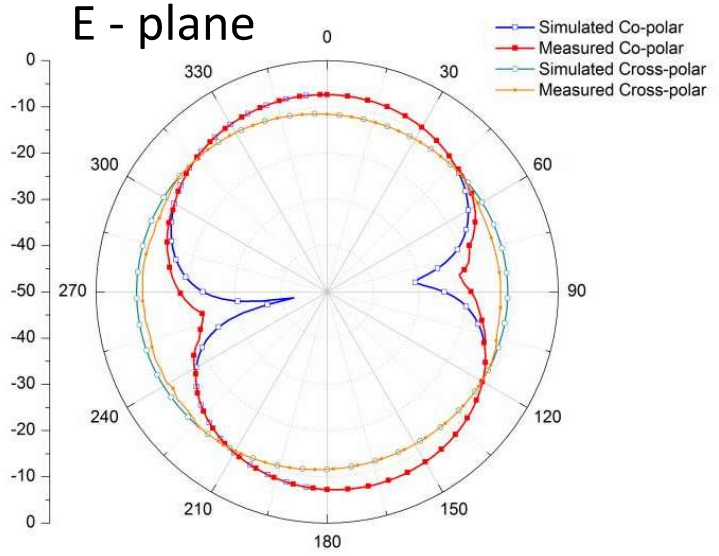


H - plane

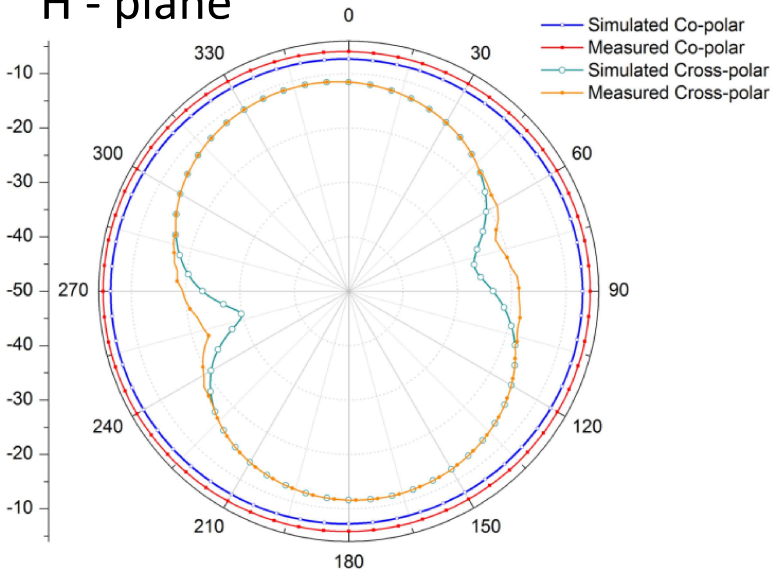


Omnidirectional pattern with Beamwidth of 90° with a 6° gain squint in broadside direction for E-plane pattern

Radiator currents flow in the same sense from the split ring end unto the feed.

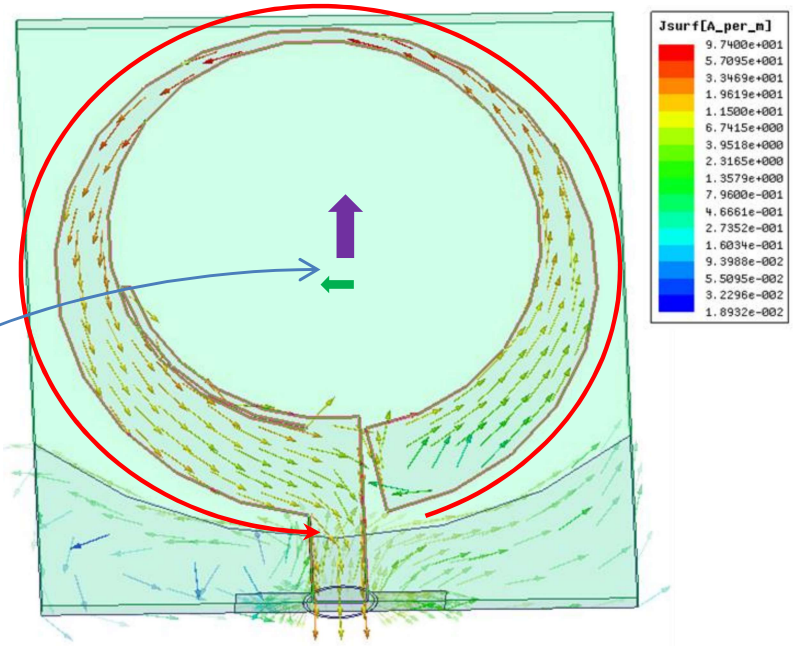


Small mutually orthogonal net current dipoles

## 2.3 Measurement Results

### Radiation Pattern at wideband resonance (3.17 GHz)

E - plane

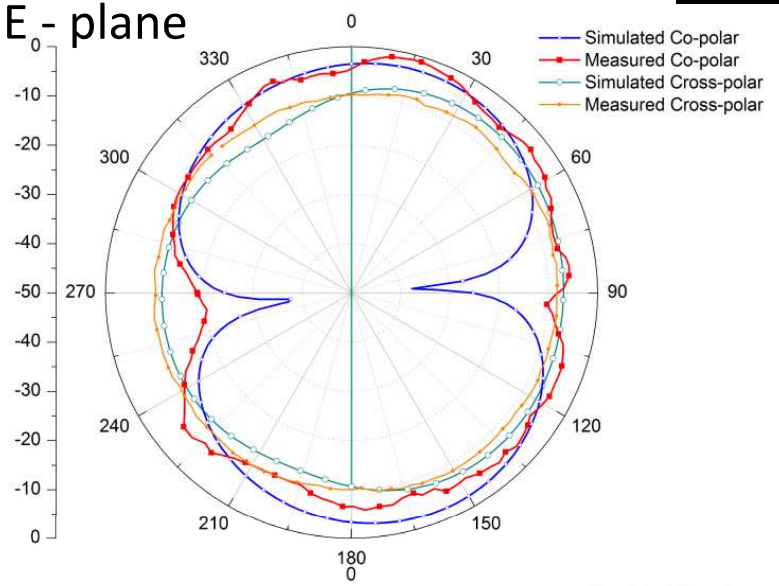


H - plane

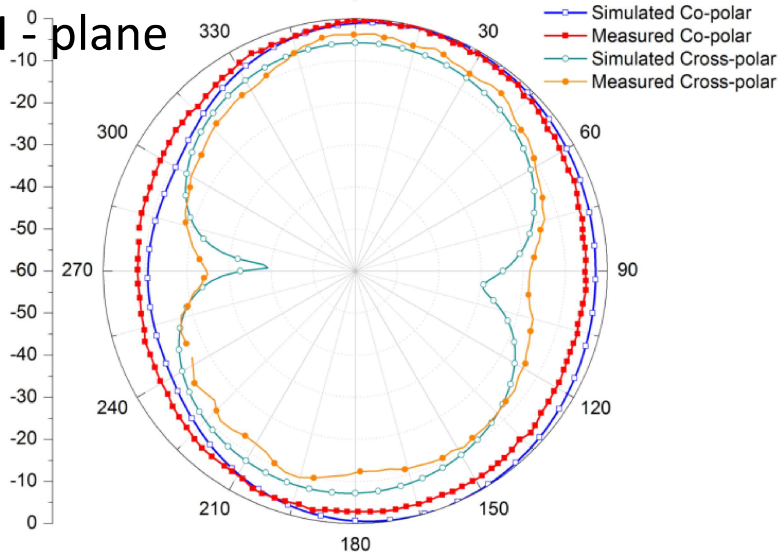


Omnidirectional pattern with Beamwidth of 78° with a 2° gain squint in broadside direction for E-plane pattern

Radiator currents flow in the same sense above a horizontal imaginary margin. This generates a net vertical current dipole, and provides an improvement in boresight directivity.

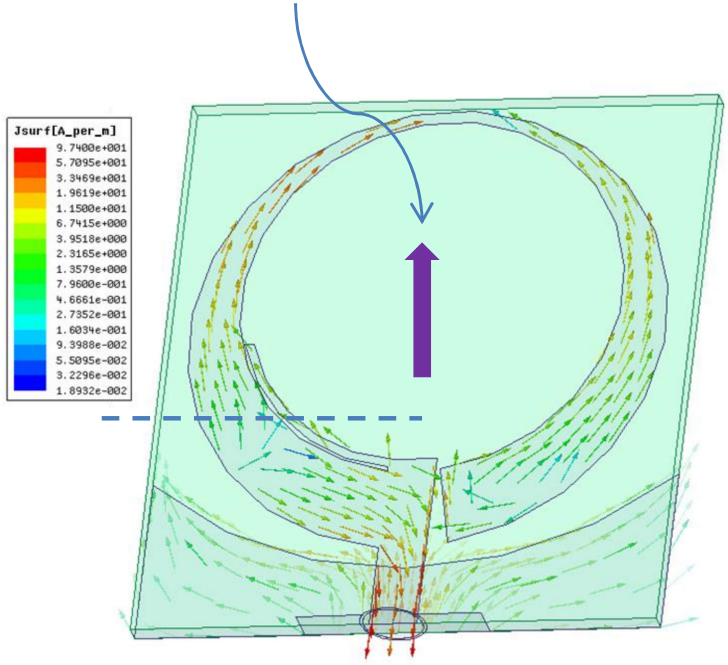

## 2.3 Measurement Results

### Radiation Pattern at band-reject frequency (2.44 GHz)

E - plane

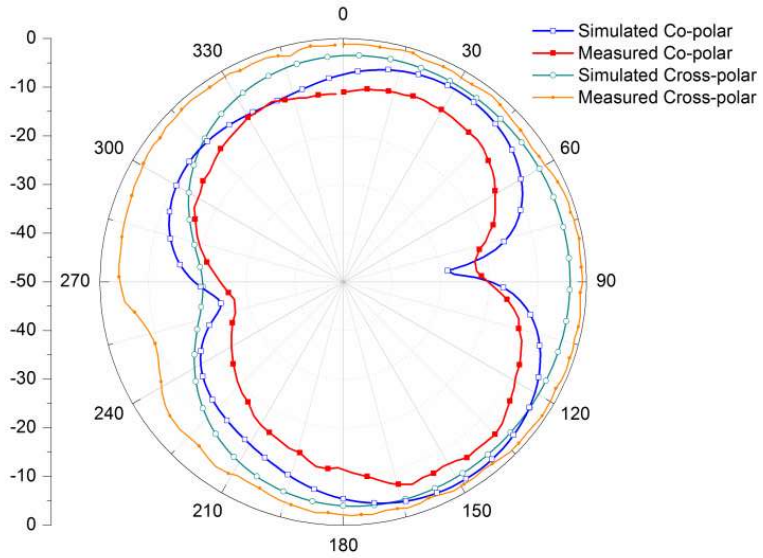


Cross-polar component envelopes co-polar component in E-plane

H - plane

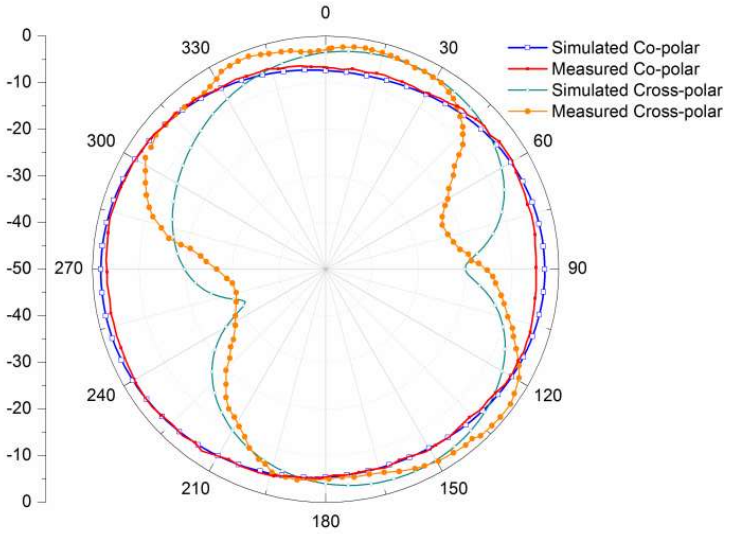


Radiator currents established on the narrower feed section are more intense in magnitude. This generates a net horizontal current dipole, and aids the cross-polar component

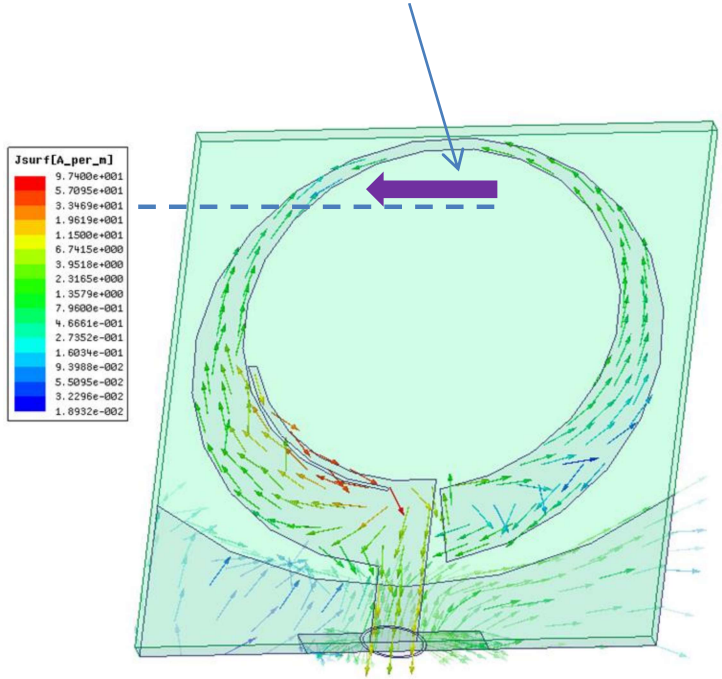

## 2.3 Measurement Results

### Gain

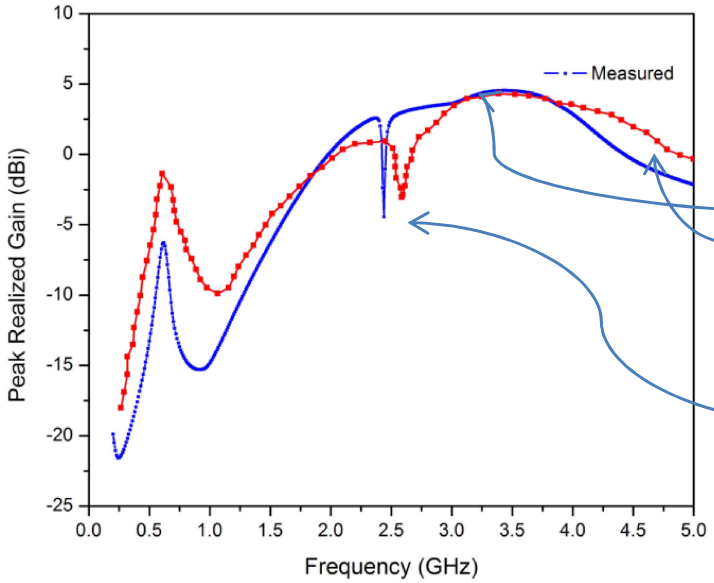


Gain lies within 4.53 dBi and shows an increasing trend.

Peak Gain of 4.53 dBi around 3.2 GHz.

Gain starts to taper off at higher frequency.

Sharp dip at 2.44 GHz – Band-reject frequency

### Radiation Efficiency

Sub-peak of 88% at 630 MHz

Peak efficiency of 91% at 2 GHz, and a gradual decrease to 75% around 4.43 GHz.

Sharp dip at 2.44 GHz to 61% – Band-reject frequency

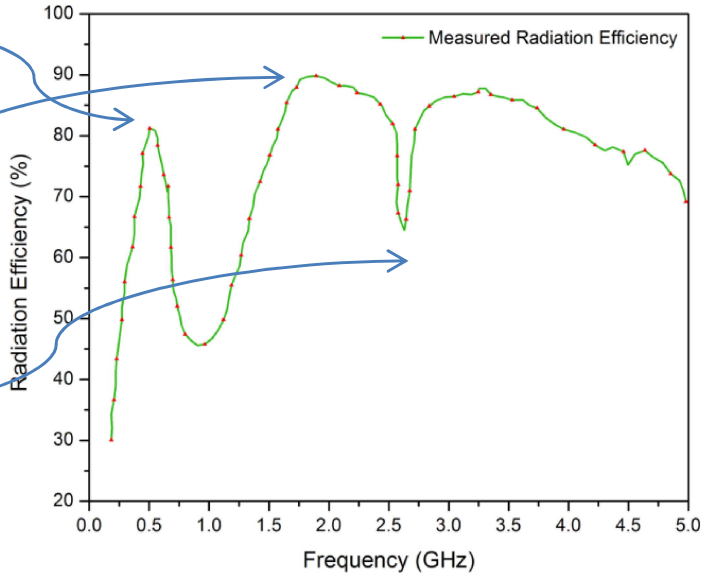

## 2.4 Comparative Analysis

| Reference | Lowest Resonant Frequency (MHz) | Substrate Permittivity $\varepsilon_r$ | Geometrical Antenna Dimensions (mm x mm) | Geometrical Area (A) ($mm^2$) | $A_{eff}$ : $\nu_{0,1}$ ($mm^2$/MHz) | Functionality, Topology |
|---|---|---|---|---|---|---|
| C.-L. Hu et al. (2010) [6] | 663 | 8.6 | 96 x 11.2 (Radiator) + 240 x 210 (Ground) | 51,475.2 | 77.64 | Quad band, PIFA |
| K.-L. Wong et al. (2013) [7] | 698 | 4.4 | 45 x 10 (Radiator) + 200x150 (Ground) | 30,450 | 43.62 | Tri band, PIFA |
| Y.-L. Ban et al (2013) [8] | 824 | 4.4 | 29 x 15 (Radiator) + 115 x 50 (Ground) | 6,185 | 7.5 | Dual Band, PIFA |
| B.S.-Izquiedo et al. (2013) [9] | 700 | 2.7 | 81.4 x 68.6 | 5586 | 7.98 | Tri band, Standalone |
| S. Ahmed et al (2015) [2] | 870 | 3.5 | 70 x 70 | 4,900 | 5.632 | Quad band, Standalone |
| *Proposed* | **630** | **2.2** | **48 x 44** | **2,112** | **3.46** | Wideband, with **Band-** |

## 2.5 Summary

- The antenna realizes a narrowband (40 MHz) match at 630 MHz due to a the ring's circumferential length.

- Wideband operation (2 – 4.23 GHz) obtained due to width of the annular ring.

- Curved ground plane structure has been found to be a key contributor in effecting the desired impedance match characteristics by proper tailoring feed gap capacitances.

- Sleeve length variations were found useful to provide band-reject characteristics in the wideband impedance match zone.
  - Significantly, it was found that the band rejections did not disturb the existing cut-in and cut-off frequencies of the existing wideband match.
    - This inspires us to investigate miniaturization potential in simple geometries by only varying their respective dimensions.
    - Also, higher cross-polarization levels in the current design motivate use of a *long-board* configuration for its improvement in its radiation patterns.
    - Lastly, a wideband coverage over maximum LTE spectrum is preferred.

# 3. Rectangular Disc Wideband Antenna

Objective

To achieve wideband coverage over most of the LTE spectrum on low permittivity substrate

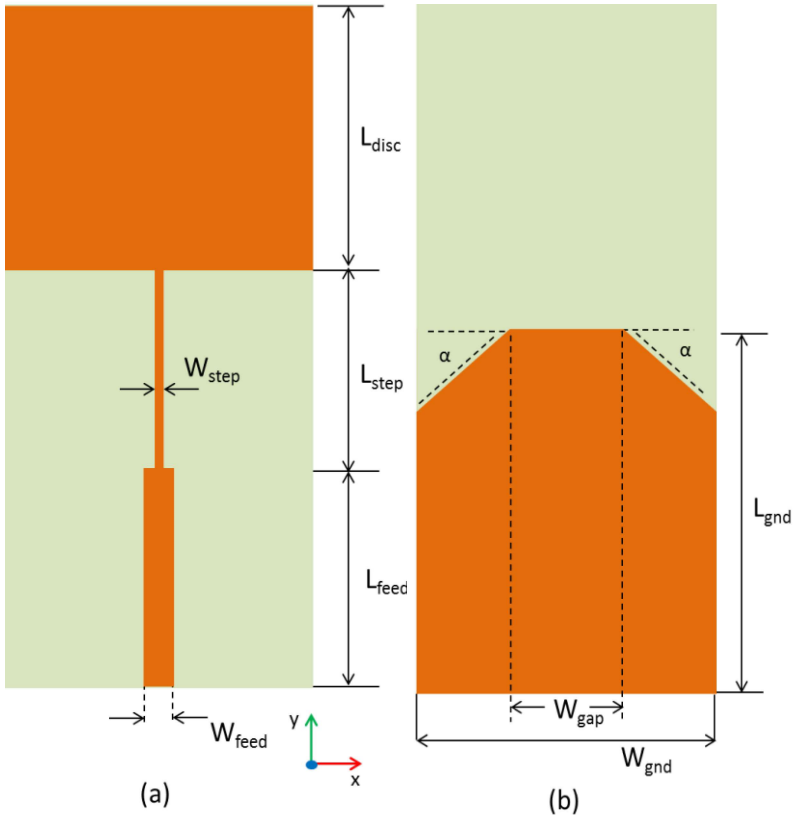


(a) Top view and (b) Rear View of the Wideband antenna

Initial structure was of a long ground plane and a rectangular disc connected to a 50 Ω microstrip feed

| Parameter | $L_{feed}$ | $L_{gnd}$ | $L_{disc}$ | $L_{step}$ | $W_{feed}$ | $W_{gnd}$ | $W_{gap}$ | $W_{step}$ |
|---|---|---|---|---|---|---|---|---|
| Values (mm) | 30 | 55 | 45 | 30 | 3 | 40 | 16 | 1.5 |
| Normalized to $\lambda_g$ | 0.16 | 0.27 | 0.23 | 0.16 | 0.016 | 0.21 | 0.08 | 0.008 |

# 3.1 Parametric Simulations and Design modification

Disc Length variations reveal lower resonance frequencies converging around 1 GHz

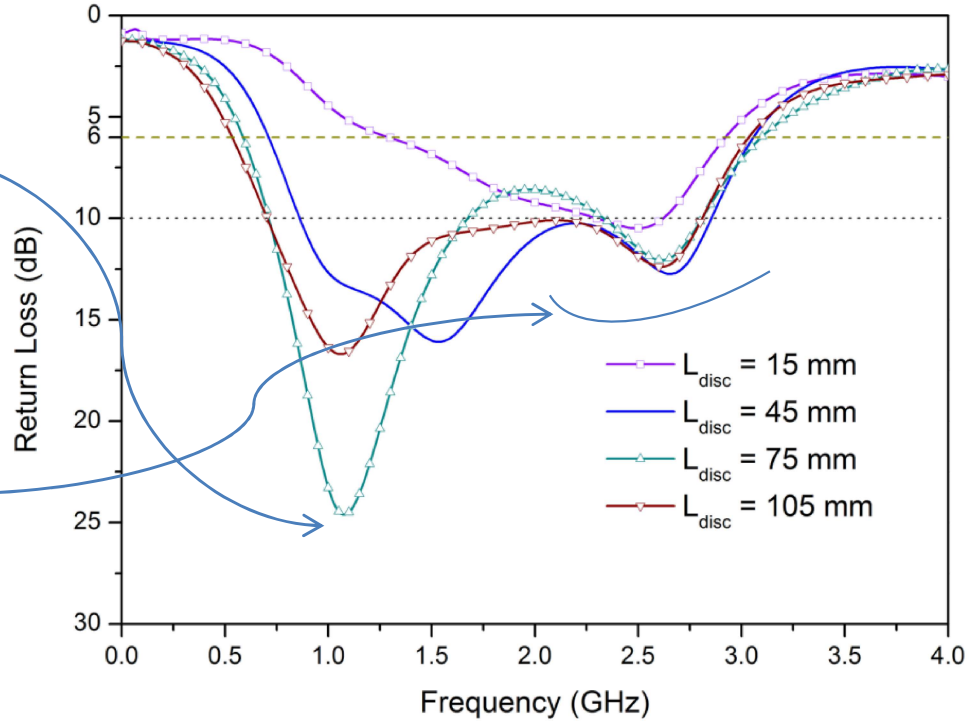


No significant variation for higher frequencies

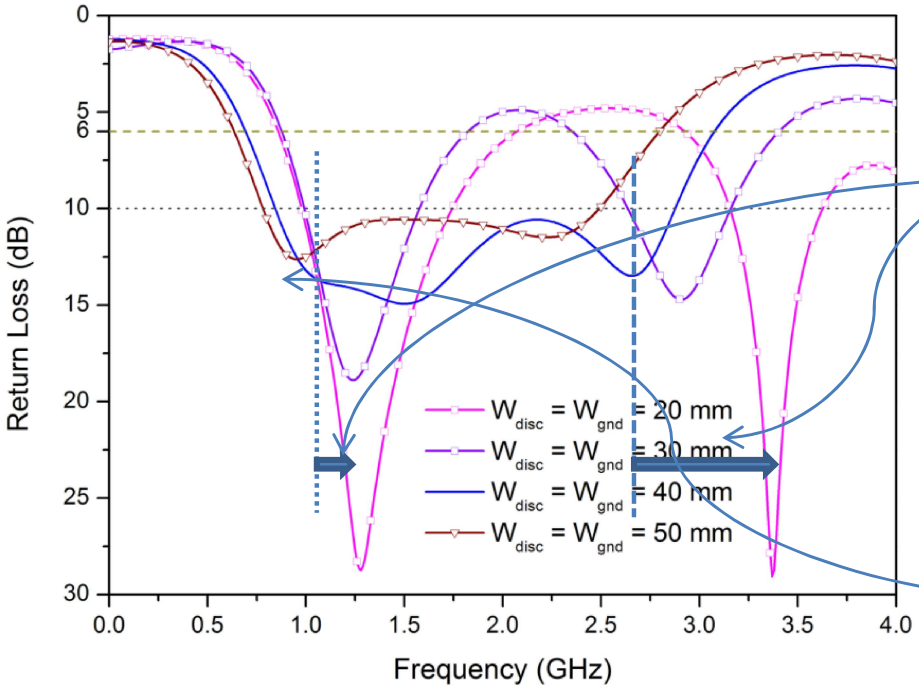


Board width reduction move characteristics upwards

Lower resonance is seen to move downwards for wider board width

# 3.1 Parametric Simulations and Design modification

Feed gap change with radiator disc length variation

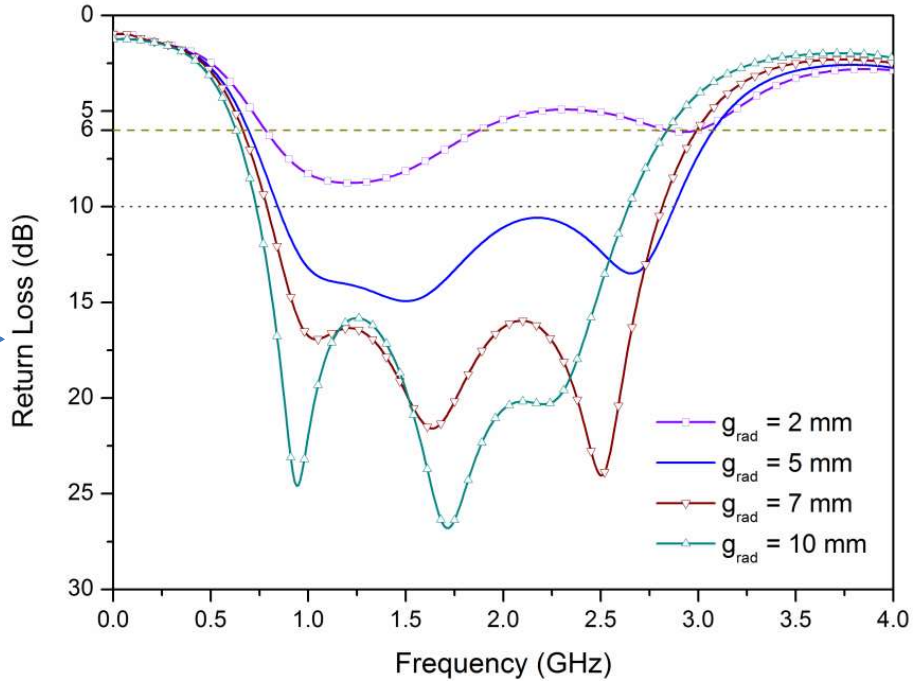


Improved impedance match with increase in Feed gap

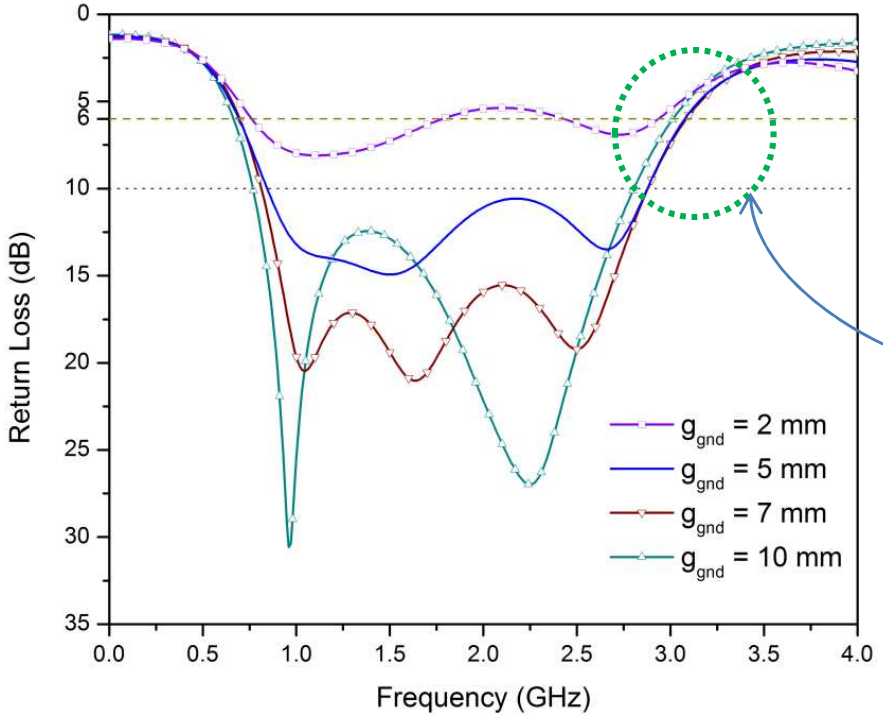


Feed gap change with ground plane length variation

Better higher cut-off frequency for increased feed gaps

## 3.1 Parametric Simulations and Design modification

Ground plane <u>bevel angle (α)</u> variation

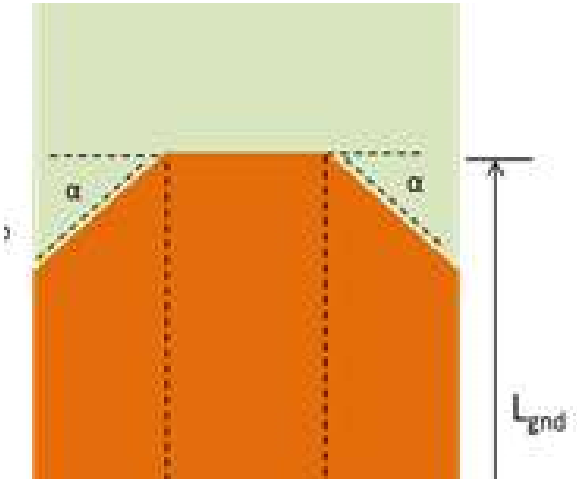


Reduction in upper cut-off frequencies with smaller bevel angles: lesser variation in feed gap capacitances with smaller bevel angles

Increased mismatch in mid-frequency band with larger bevel angles

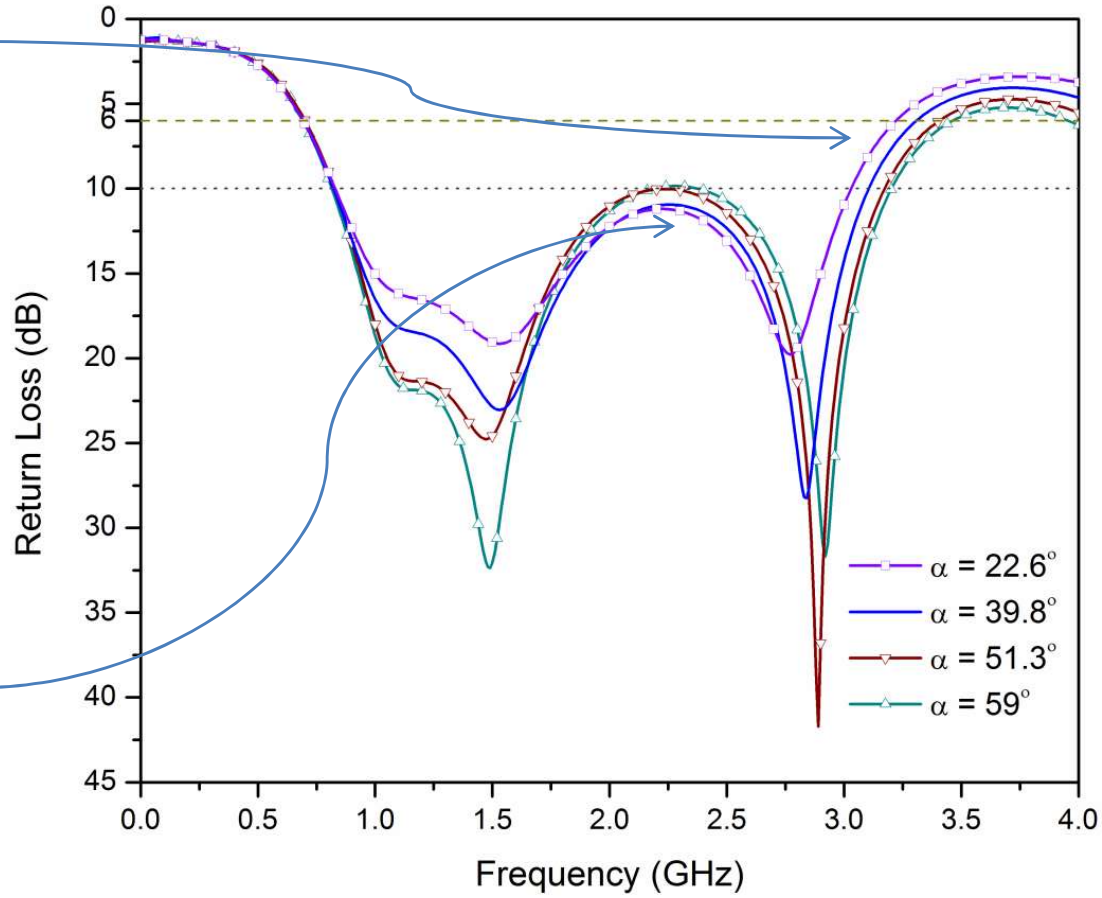

## 3.2 Measurement Results

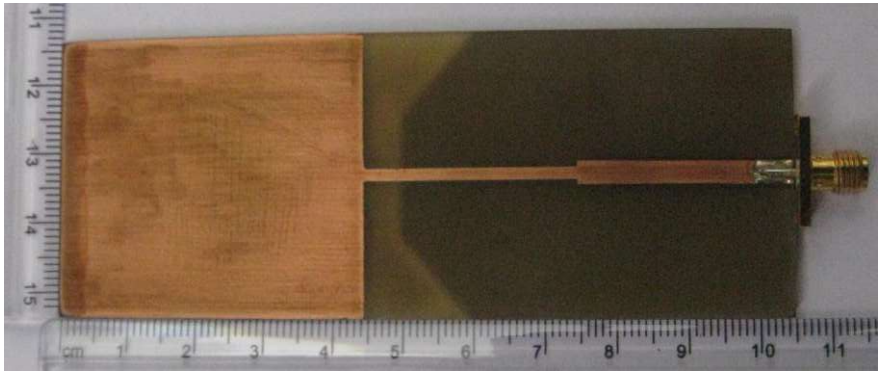

(a) Top view of the fabricated antenna

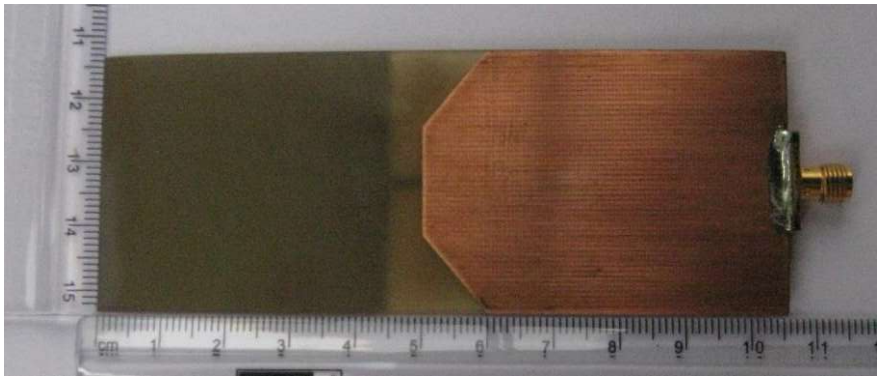

(b) Rear view of the fabricated antenna

The annular split ring multiband antenna prototype is fabricated fabricated on a 1/16" (1.5875 mm) thick FR4 board ($\varepsilon_r$ = 4.4) of dimensions 105 × 40 mm$^2$.

### Return Loss measurements

Measured characteristics (0.7 – 3.47 GHz) follow simulation trend.

An overall gradual shift of impedance match characteristics towards higher frequencies is seen: fabrication errors likely.

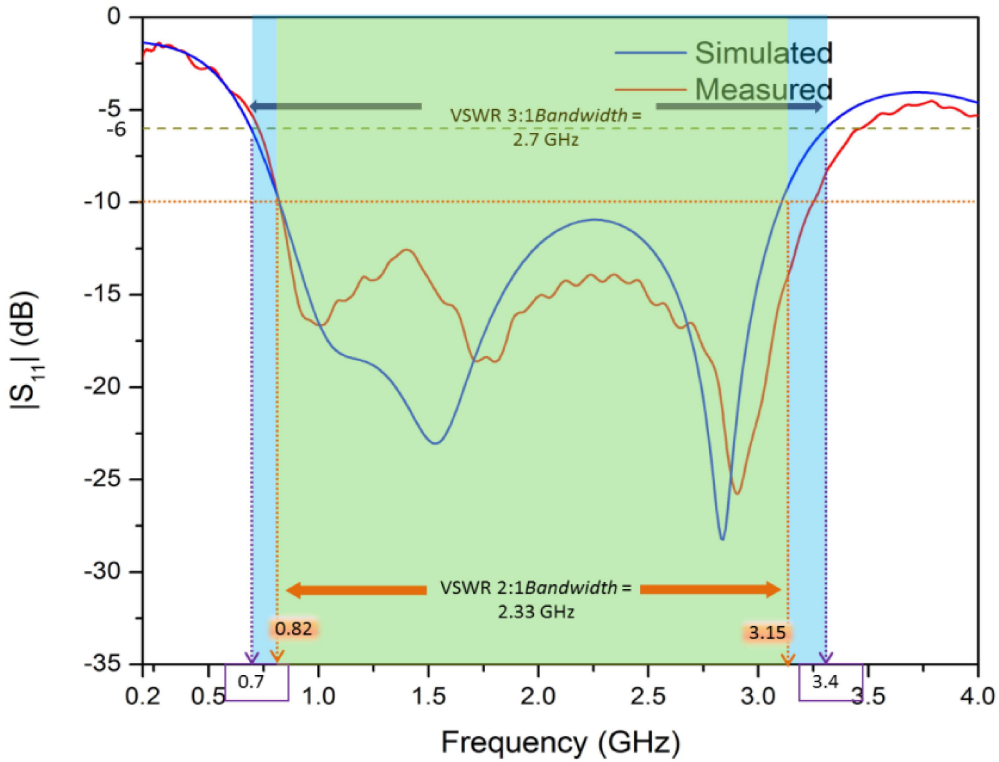

## 3.2 Measurement Results

Radiation Pattern at lower edge frequency (700 MHz)

E - plane

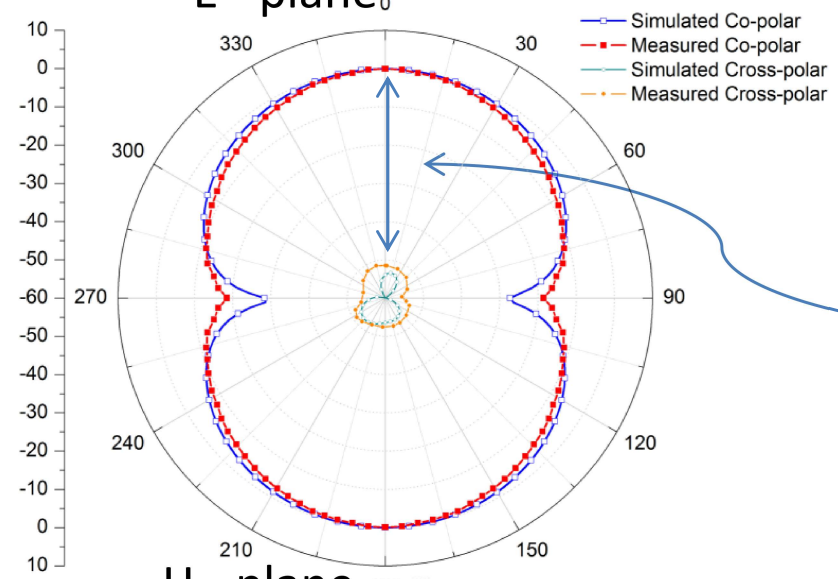


H - plane

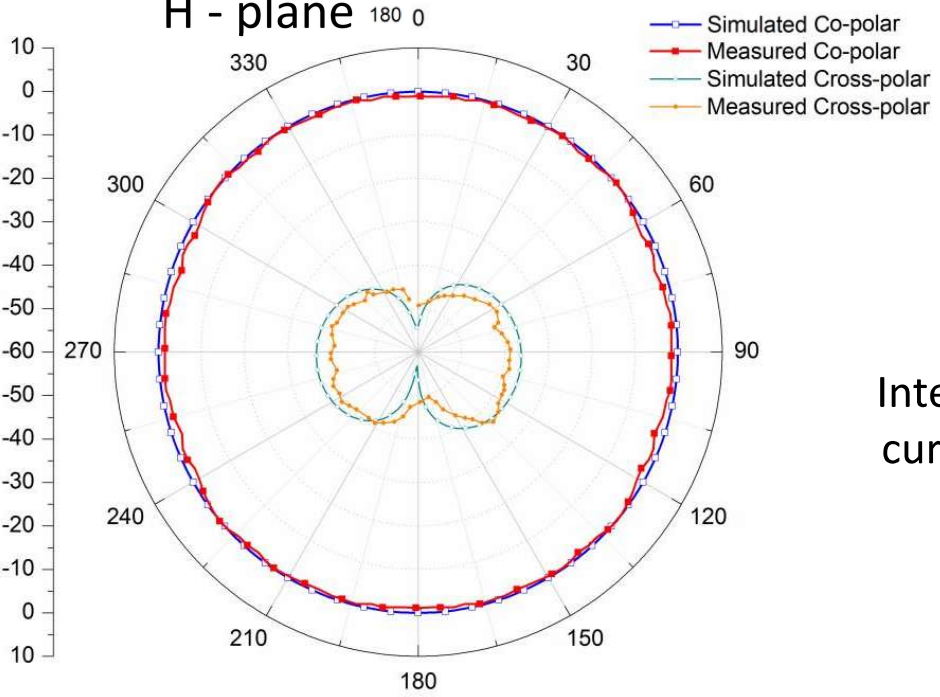


Omnidirectional pattern with Beamwidth of 88° with radiation in broadside direction for E-plane pattern

Highly reduced cross-polar levels. Cross-polar discrimination: 52.3 dB (E-plane), and 38.4 dB (H-plane): virtue of long-board configuration

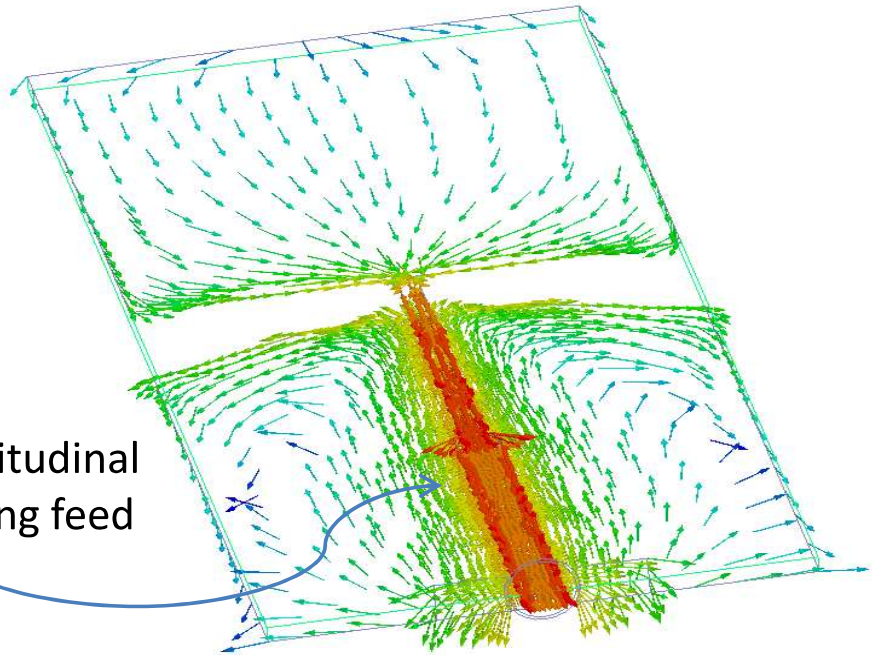

Intense longitudinal currents along feed

## 3.2 Measurement Results

### Radiation Pattern at upper edge frequency (3.4 GHz)

E - plane

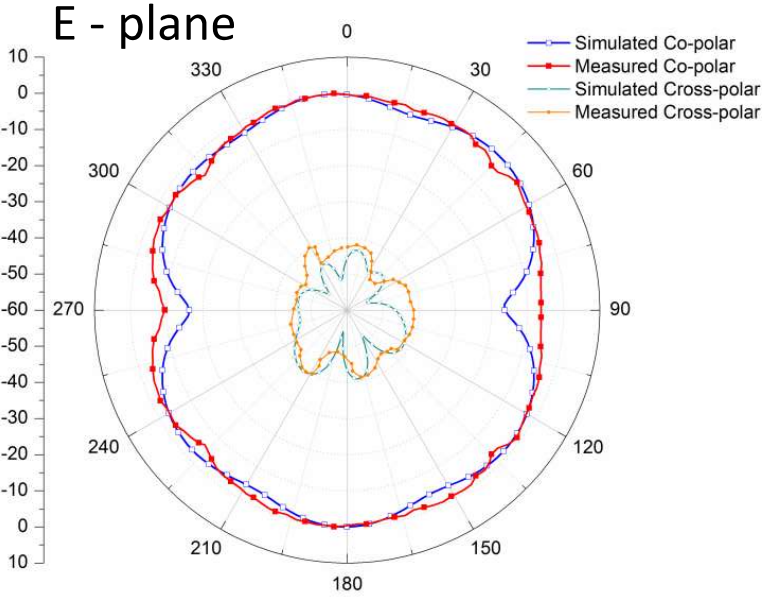


Omnidirectional pattern with Beamwidth of 40° with radiation in broadside direction for E-plane pattern: more lobulated.
H-plane pattern becomes oblong.

Reduced cross-polar levels. Cross-polar discrimination: 34.8 dB (E-plane), and 25.83 dB (H-plane)

H - plane

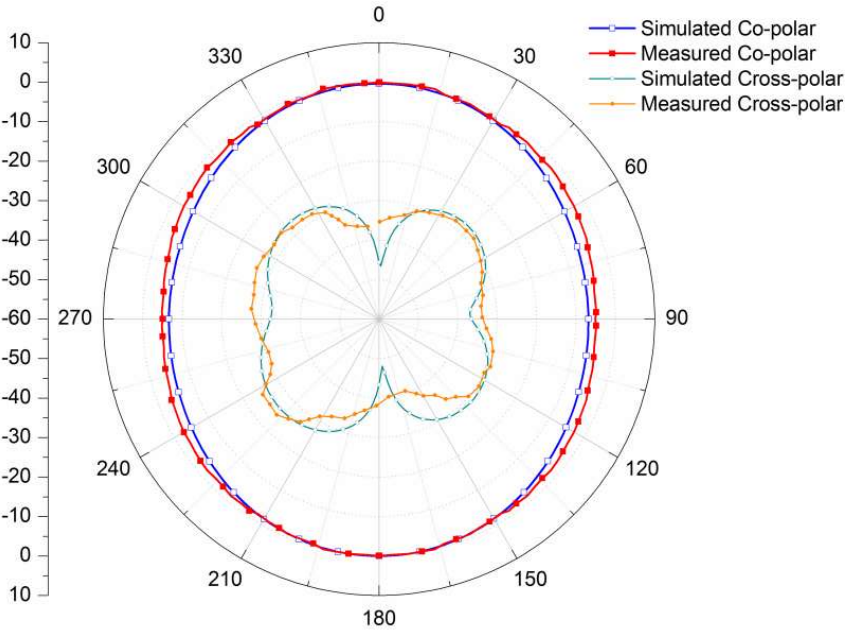


Higher order modes develop along feed line

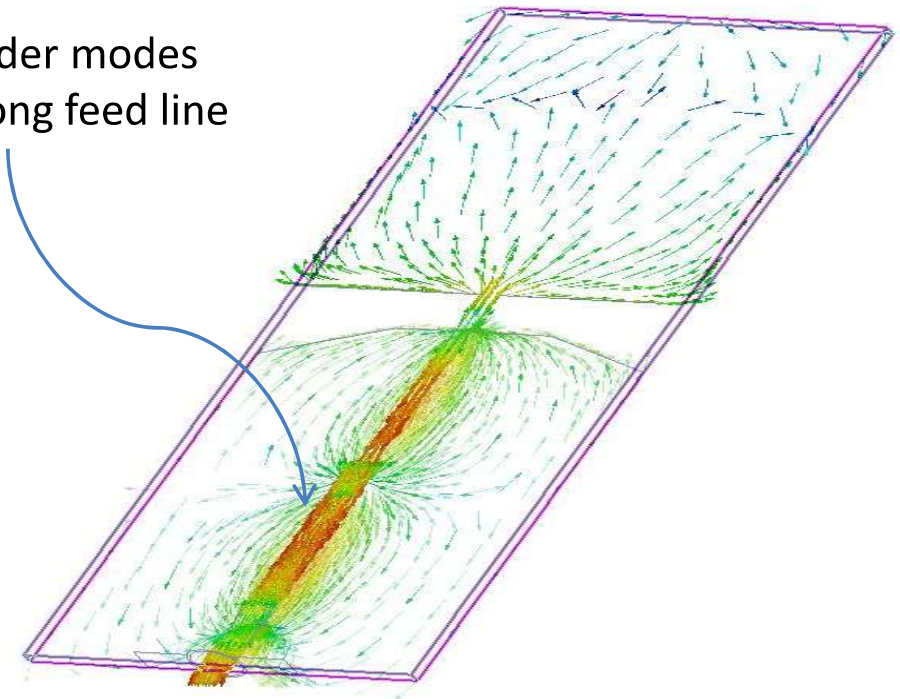

## 3.2 Measurement Results

### Gain

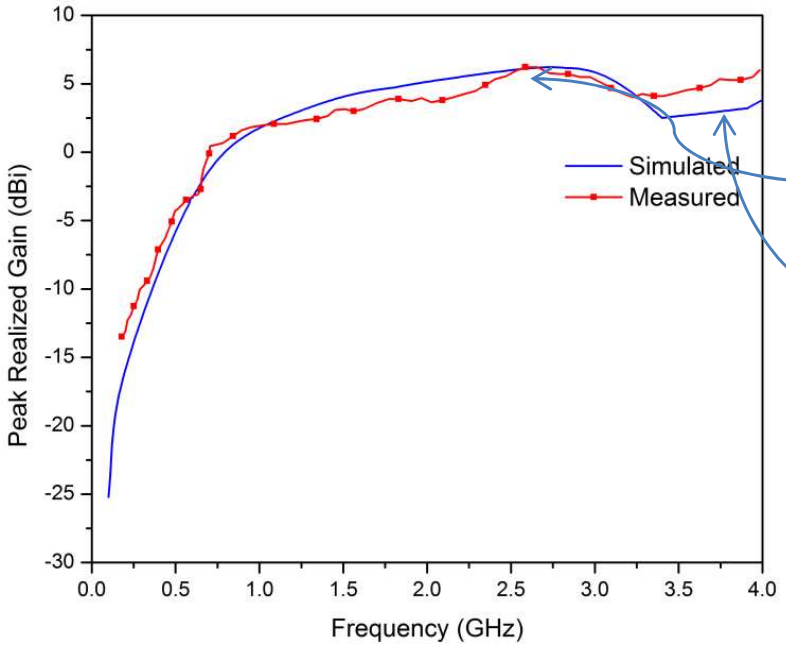


Gain lies within 6.2 dBi and shows an increasing trend.

Peak Gain of 6.2 dBi around 2.67 GHz (best impedance match)

Gain starts to taper off at higher frequency.

### Radiation Efficiency

Peak efficiency of 92% at 0.7 GHz, and a gradual decrease to 76.5% around 3.4 GHz.

Sharp rise at low frequency due to monotonic improvement in impedance match

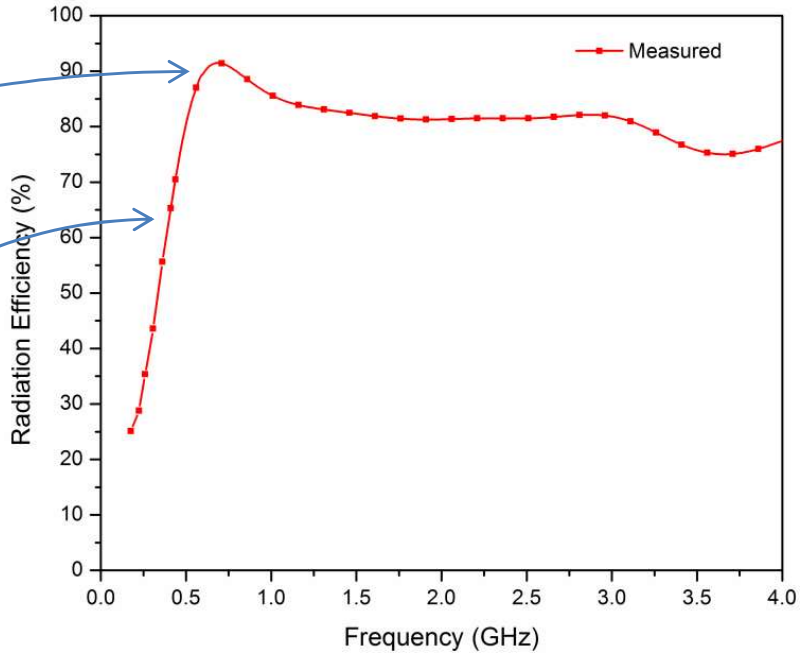

## 3.3 Comparative Analysis

| Reference | Lowest Edge Frequency (GHz) | Fractional Bandwidth (%) | Substrate Permittivity $\varepsilon_r$ | Geometrical Antenna Dimensions L x W (mm x mm) | Effective Antenna Dimensions $L\sqrt{\varepsilon_{r,avg}}$ x $W\sqrt{\varepsilon_{r,avg}}$ (mm x mm) | Effective Antenna Area ($mm^2$) | Effective Area: Fractional Bandwidth Ratio ($mm^2$) |
|---|---|---|---|---|---|---|---|
| W.-S. Chen et al (2010) [4] | 0.53 | 139.9 | 4.4 | 200 x 40 | 328.6 x 65.73 | 21,600 | 132.09 |
| J. Liu et al (2011) [5] | 1.08 | 184.83 | 3.48 | 124 x 120 | 185.6 x 179.6 | 33,331 | 180.33 |
| Z. Guo et al (2013) [6] | 1.67 | 151 | 4.4 | 115 x 60 | 189 x 98.6 | 18,630 | 123.377 |
| S.-Li Zuo et al (2013) [1] | 0.44 | 101.7 | 4.4 | 200 x 44 | 225.2 x 72.3 | 16,280 | 160.08 |
| M.H. Rabah et al (2015) [8] | 0.67 | 178.84 | 10.2 | 68 x 33 | 160.91 x 78.1 | 12,566 | 70.27 |
| ***Proposed*** | 0.7 | 131.7 | **4.4** | 105 x 40 | 172.5 x 65.73 | **11,340** | 86.105 |

Poor Radiation Efficiency -
~ 25% around 700 MHz

## 3.4 Summary

- It was found that for a given width of the ground plane, the lowest resonant frequency cannot be decreased further despite any increase in length of the radiator disc.

- Impedance match characteristics have been found to be very sensitive to feed gap variations.

- Feed gap variations induced by ground plane length adjustments are better than radiator length adjustments as they do not perturb the upper cut-off frequencies of the wideband impedance match.

✓ Extremely good cross-polar discrimination and radiation efficiency is obtained over the operational spectrum.

✓ A very good optimization is observed as lesser area is required to provide a very wide bandwidth (fractional bandwidth: 131.7%)

➢ However, time-consuming and iterative optimizations motivate the need to find a less complex, mathematical technique for antenna design, albeit for simpler geometries.

# 4. Transmission line based Stepped Wideband Antenna

Objective

To extend theoretical framework of transmission lines for designing a wideband antenna and regulate impedance match characteristics with ground plane based stubs

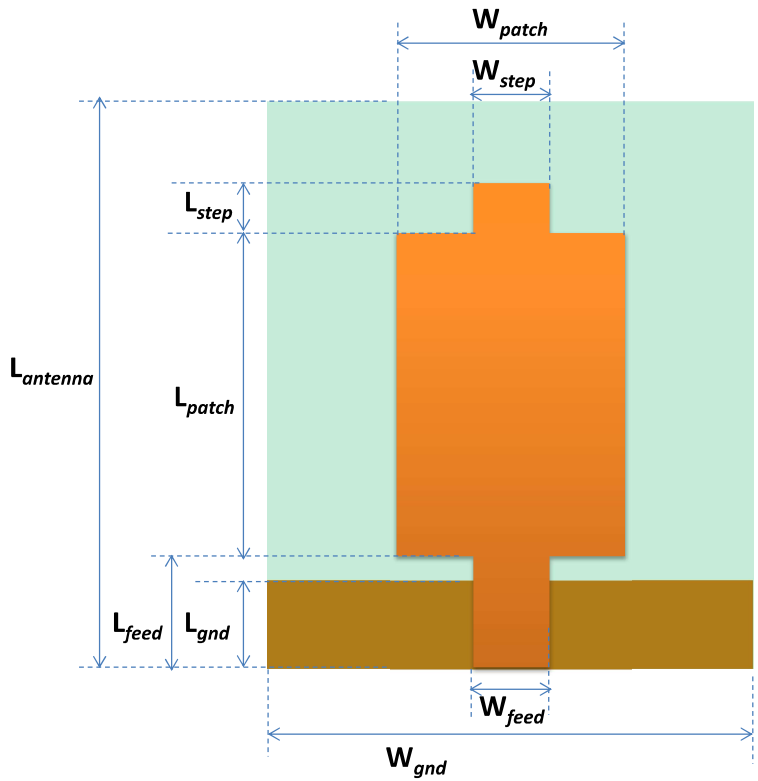


| Parameter | $L_{feed}$ | $L_{antenna}$ | $L_{gnd}$ | $D_{stubs}$ | $L_{step}$ | $L_{patch}$ | $W_{step}$ |
|---|---|---|---|---|---|---|---|
| Values (mm) | 7 | 35 | 5.5 | 5 | 3 | 20 | 4.7 |
| Parameter | $W_{feed}$ | $W_{gnd}$ | $W_{patch}$ | $W_{S\_stub}$ | $W_{C\_stub}$ | $H_{C\_stub}$ | $H_{S\_stub}$ |
| Values (mm) | 4.7 | 30 | 14 | 1 | 6 | 0.2 | 2 |

# 4.1 Modeling of initial Wideband Antenna

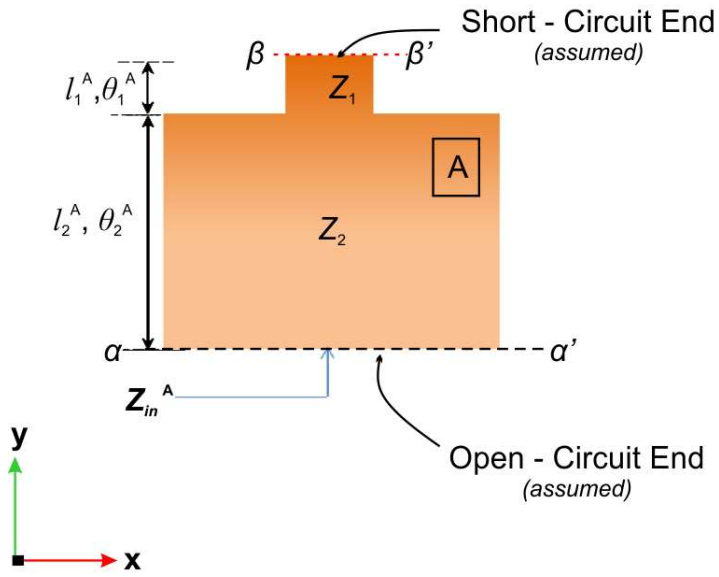


Consider top section of the antenna

$$Z_{in} = jZ_2 \frac{Z_1 \tan\theta_1 + Z_2 \tan\theta_2}{Z_2 - Z_1 \tan\theta_1 \cdot \tan\theta_2} \approx 0 \qquad (1)$$

➔ Resonance

At 1st resonance, $f_{o,1}$ : $$Z_2 = Z_1 \tan\theta_1 \cdot \tan\theta_2 \qquad (2)$$

At 2nd resonance, $f_{o,2}$ : $$\tan(R_f\theta_1) \cdot \tan(R_f\theta_2) = Z_2 / Z_1 = R_z \qquad (3)$$

Where $R_f = v_{o,2} / v_{o,1}$ is the resonance frequency ratio

- Since same structure should support both resonances, (2) and (3) are solved together:

$$\tan(R_f\theta_1) \cdot \tan\left[ R_f \tan^{-1}\left( \frac{R_z}{\tan\theta_1} \right) \right] = R_z \qquad (4)$$

# 4.1 Modeling of initial Wideband Antenna

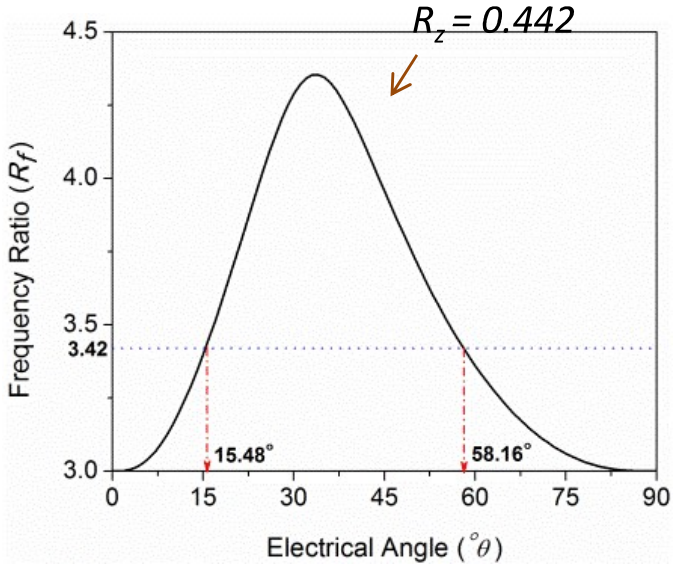


(4) is solved implicitly for the designer's choice of $R_z$, and solution obtained as a plot between $R_f$ and θ

**Target : FCC UWB Band**

$\nu_{o,1}$ = 3.1 GHz, $\nu_{o,2}$ = 10.6 GHz,

| .: For $R_z$ = 0.442 | |
|---|---|
| ($\theta_1$, $\theta_2$) | (15.48°, 58.16°) |

2nd Section (Section B) lengths $l_1^B$ and $l_2^B$ are obtained from their corresponding angles $\theta_1^B$ and $\theta_2^B$ by complementing the phase resonance condition at the second resonance point, $f_{o,2}$.

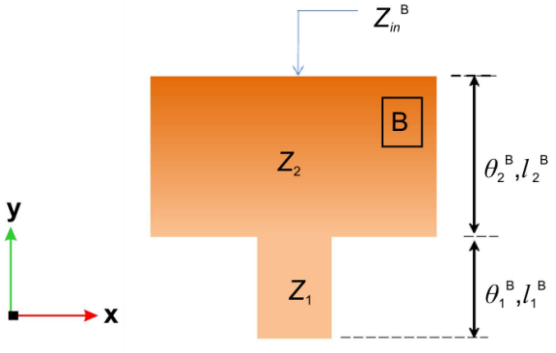


$$R_f\theta_2^B = 2\pi - R_f\theta_2^A \qquad (5)$$

$$R_f\theta_1^B = \pi - R_f\theta_1^A \qquad (6)$$

# 4.2 Simulation of initial Wideband Antenna

**Combining both Section A and Section B generates a UWB Antenna :**

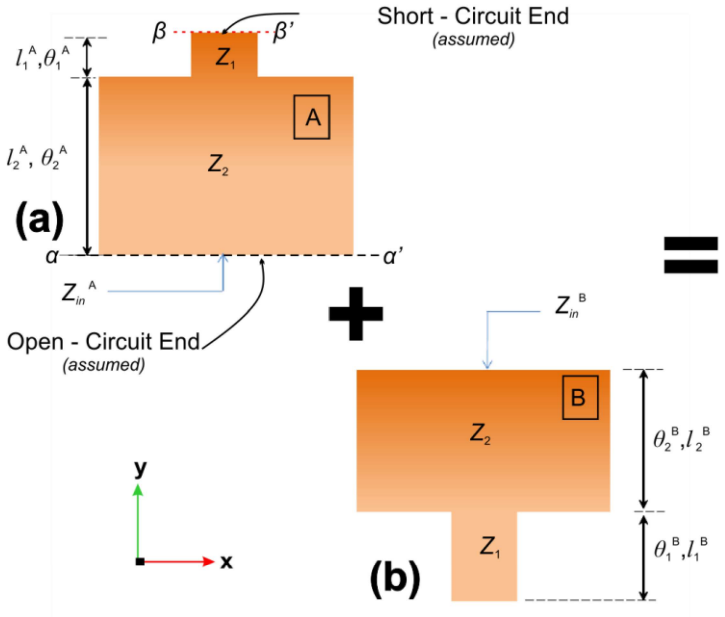


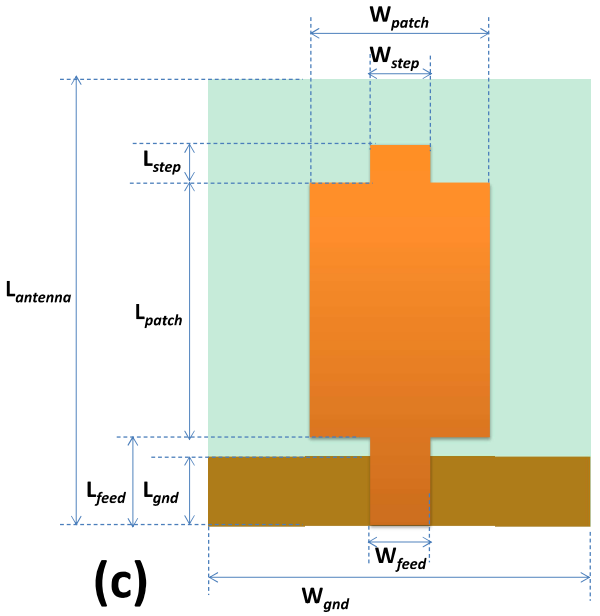


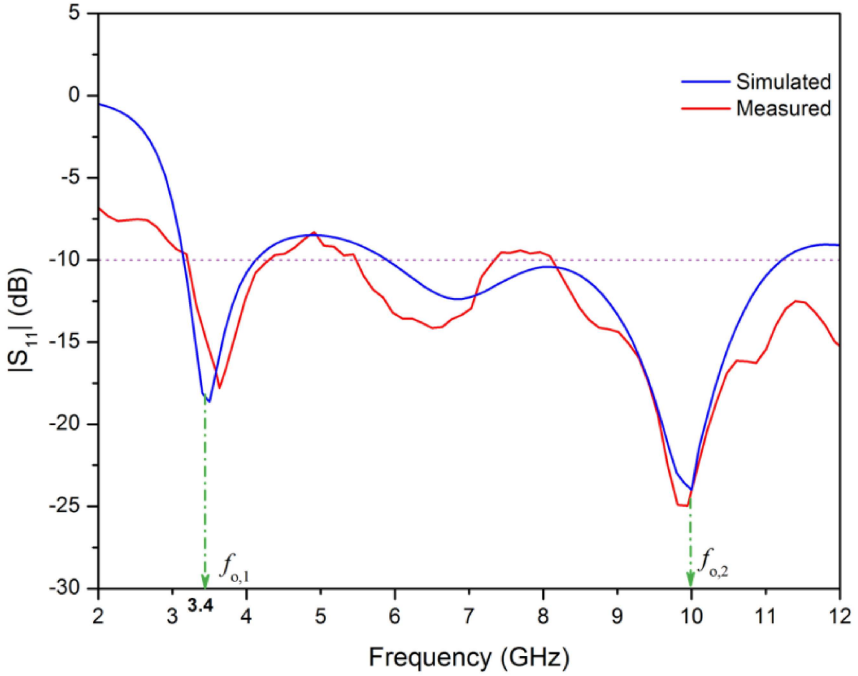


| Parameters: | $L_{step}$ | $L_{patch}$ | $L_{feed}$ |
|---|---|---|---|
| Computed (mm) | 3.0456 | 19.9923 | 7.0632 |
| Simulated (mm) | 3 | 20 | 7 |

| Resonance | First (GHz) | Second (GHz) |
|---|---|---|
| Target (Calculation-based) | $f_{R,1}$= 3.1 | $f_{R,2}$=10.6 |
| Simulated | $f_{o,1}$ =3.4 | $f_{o,2}$=10 |

# 4.2 Simulation of initial Wideband Antenna

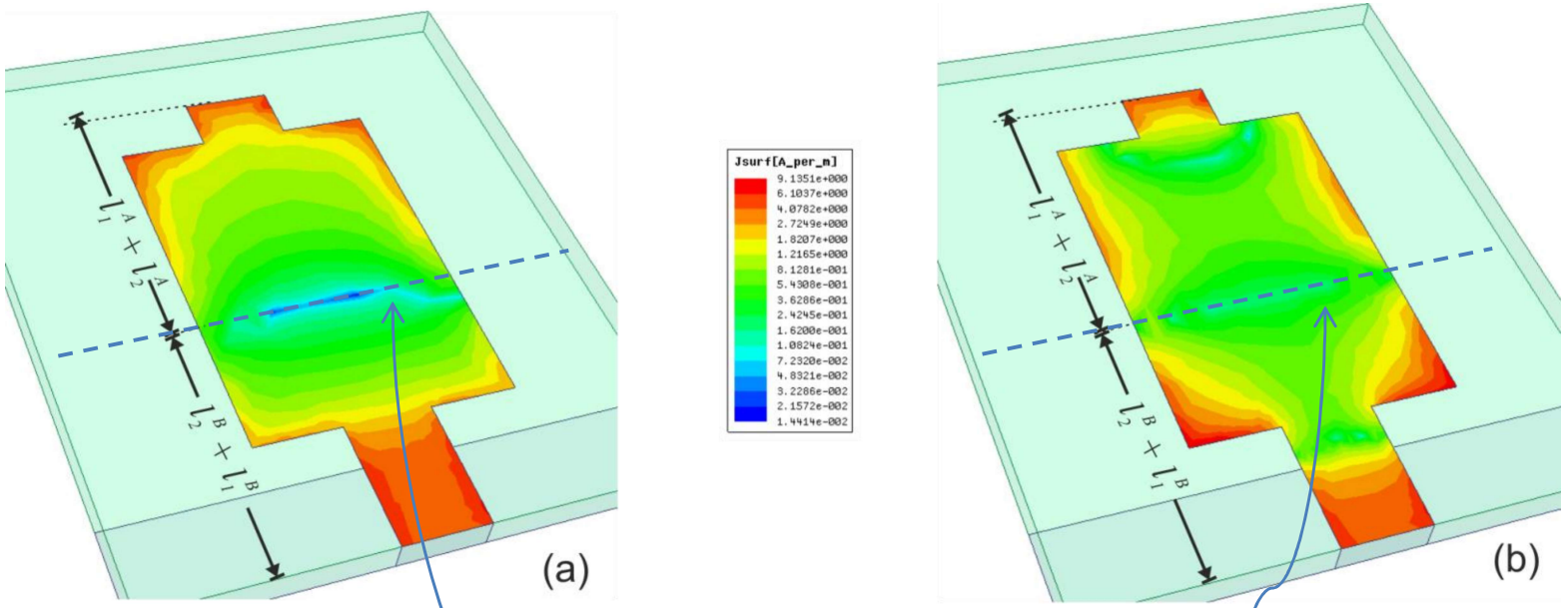


Simulated surface current distribution at (a) $f_{o,1}$= 3.4 GHz and (b) $f_{o,2}$= 10 GHz

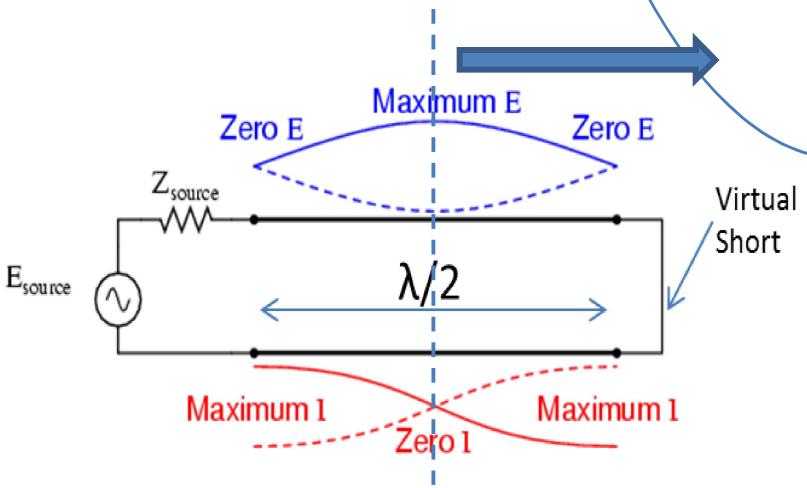


Very low current density at interface of both sections

In circuits' convention, this manifests as an open circuit

# 4.3 Ground plane stubs based tuning

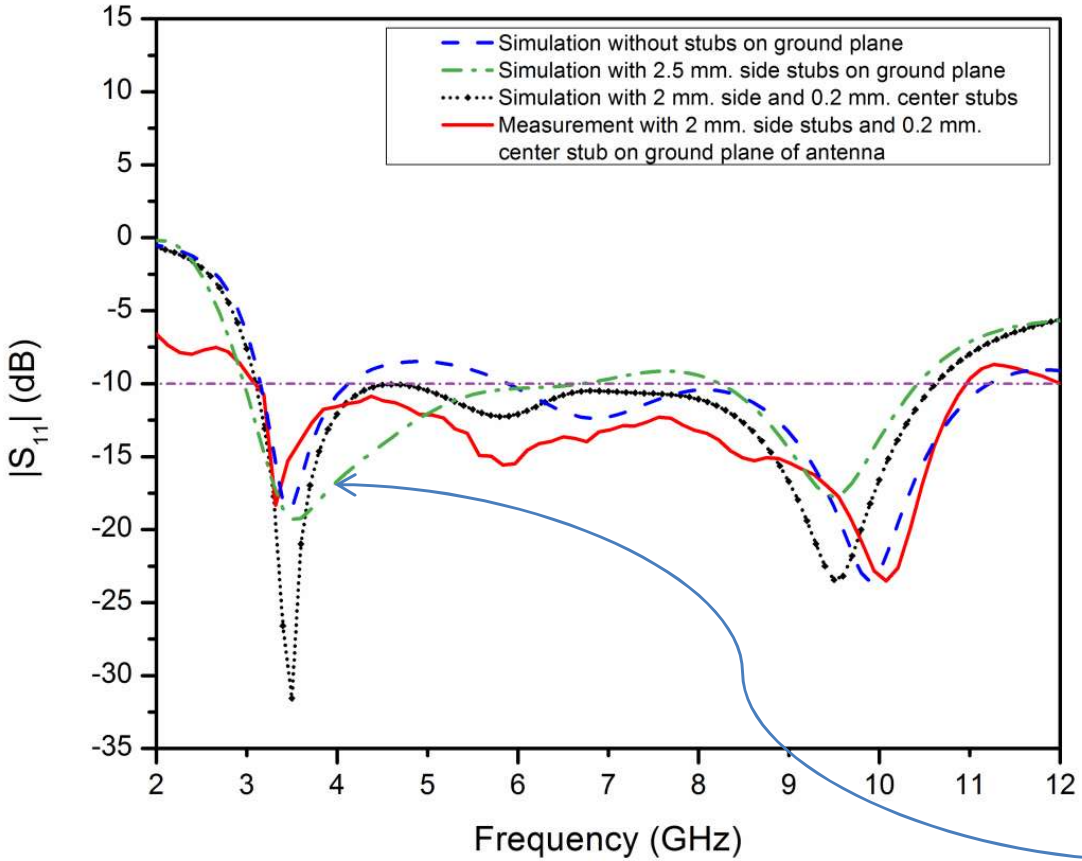


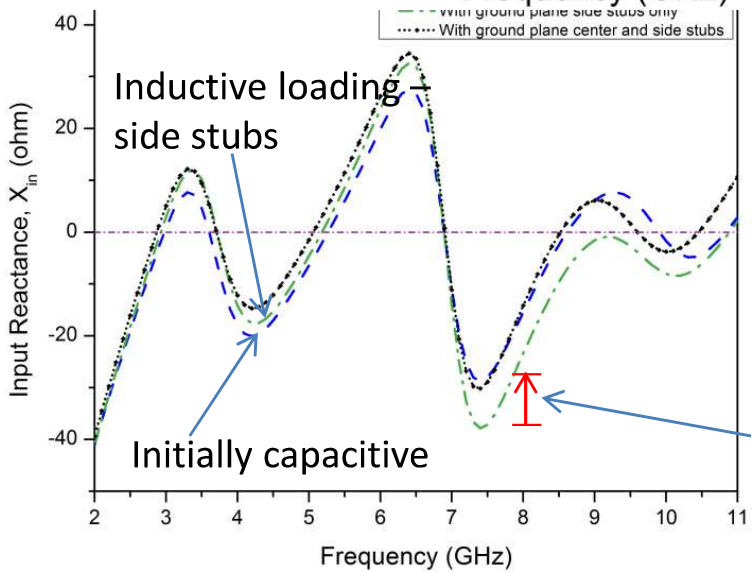


Capacitive correction by center-stub addition

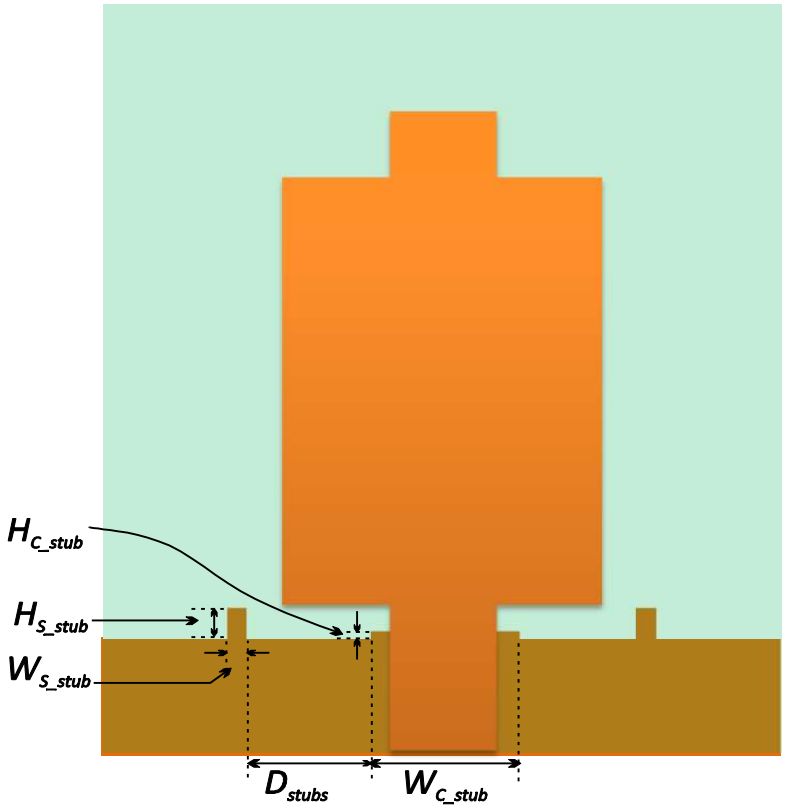


With only-Side stubs tuning, we improve low frequency match, but degrade the higher frequency match.

With a Center stub, we correct the mismatch of Side stubs in the high frequency domain.

Both Side and Center stubs balance each other out by their respective heights *in between* the resonance dips.

## 4.4 Measurement Results

Radiation Pattern at (i) first resonance (ii) intermediate frequency and (iii) second resonance

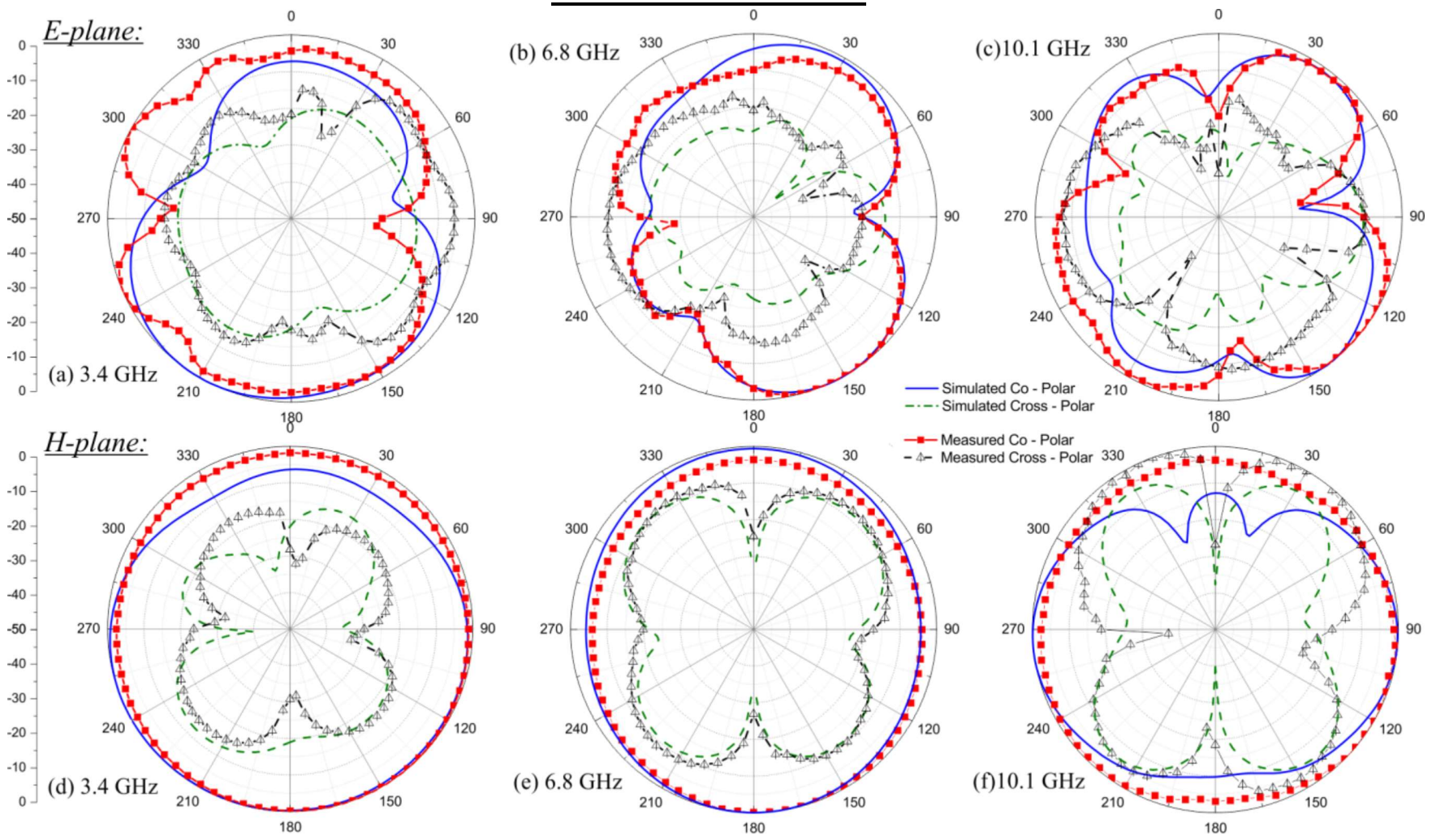


E-plane and H-plane:

Omnidirectional, but lobulated and cross-polar components increasing with frequency.

E-plane measurement: Feeder cable currents influence measurements at 90° & 270°

## 4.4 Measurement Results

### Gain & Radiation Efficiency

- Gain lies between 2.5 to 5 dBi over frequency range.
- The efficiency rises from around 90% around the lower frequency edge of the UWB band and peaks at 97% around mid-spectrum region.
- Mid-band frequencies around 6 GHz show the best gain and efficiencies.

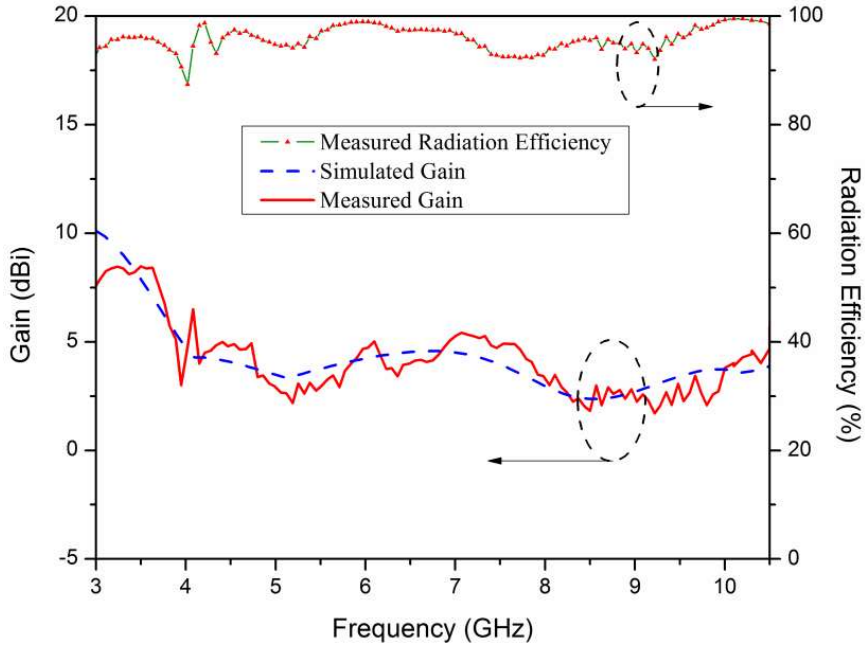


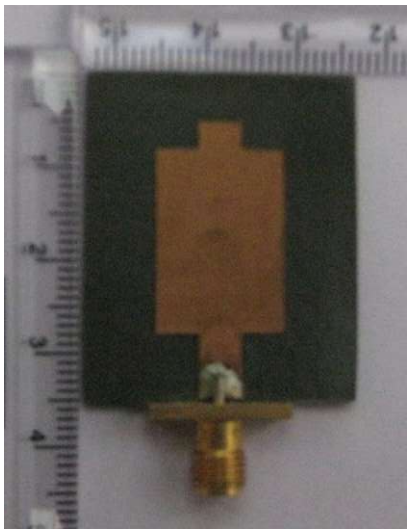

(a) (b)

(a) Top and (b) Rear View of fabricated antenna

The stepped UWB antenna prototype is fabricated on a 1/16" (1.5875 mm) thick Rogers 5008 board ($\varepsilon_r$ = 2.2) of dimensions 35 × 30 $mm^2$.

Design dimensions are as illustrated earlier in Table 1.

## 4.5 Summary

- The technique presented invokes a combination of stepped impedance resonator and phase resonance to design a dual resonant antenna.

✓ Through this effort, it has been possible to extend the earlier reported work in narrowband antenna designing over a wider bandwidth, within 9% of target frequencies.

✓ Ground plane stubs based tuning has been shown effective in fine tuning inter-resonance impedance match. This has helped render an ultrawideband coverage from 3.2 to 11.3 GHz (fractional bandwidth of 111.72 %) for the antenna.

- While the investigated technique is in a nascent stage of development and more research is required to establish its context of application, it seems to show promise of further exploration.

➢ With the small ground stubs found effecting an impedance tuning, it provokes a query if an additional ground plane can provide further regulation over impedance match. Besides, from the wideband LTE antenna in long-board configuration, we were hoping to reduce antenna dimensions but retain the cross-polar discrimination.

# 5. Stripline-fed Superstrate Topology for Antenna Miniaturization

Objective

To investigate a new topology of antenna design for miniaturization

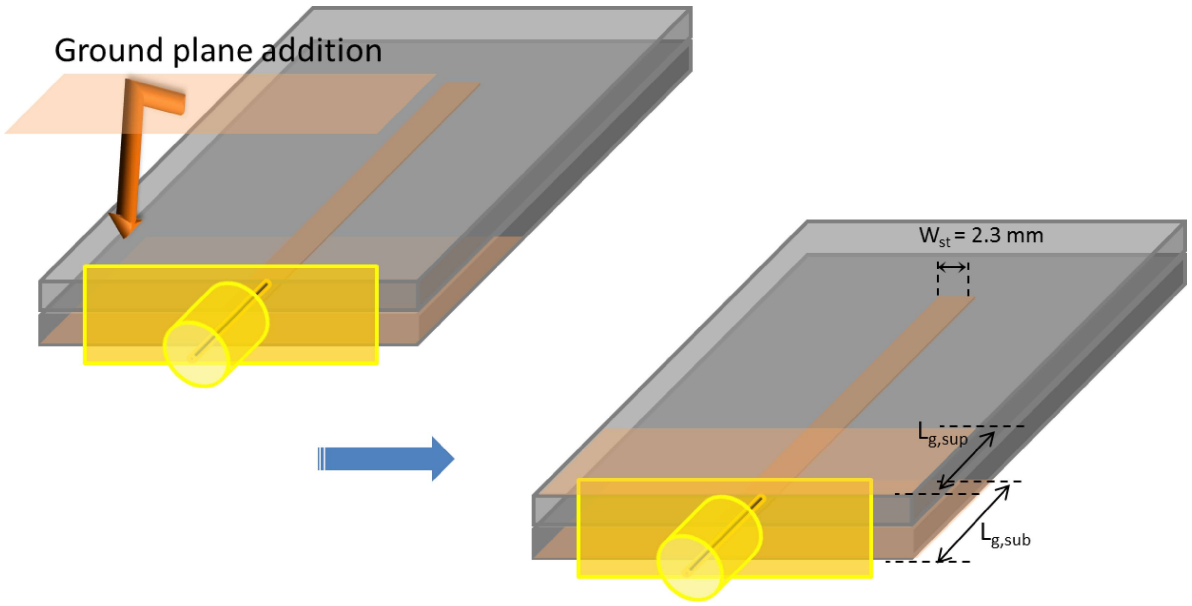


Schematic showing symbolic conversion of superstrate loaded monopole to a ‘sandwich’ strip monopole.

## 5.1 Motivation

Superstrate loaded monopoles commonly reported have heterogenous dielectric layers

Higher Dielectric constant of one layer

➔ Higher gain

➔ Asymmetric radiation patterns

Homogenous dielectric superstrates have not been popular

Stripline – fed Triangular Monopole

$\varepsilon_r$ = **3.0** (0.762 mm. thick)

➔ 37% size reduction @1.78 GHz[1]

➔ θ = 60°flare angle giving 32.5% Bandwidth

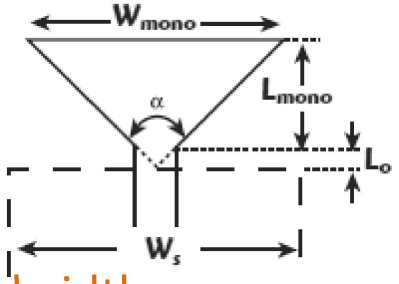


Stripline – fed Superstrate Monopole

Proposed

Extended stripline-fed substrate sandwiches radiator element + connected only at the feed port edge (SMA connector). } Unperturbed Dual Ground Planes

Study: Effects of Dual Ground planes

*(in terms of)*

Resonance shifts | Impedance bandwidth | Radiation pattern


[1] Kin-Lu Wong, Yin-Fang Lin, "Stripline-fed printed triangular monopole", Elect. Letters, Vol. 33, Issue 17, pp. 1428 – 1429 , Aug. 1997

# 5.2 Design improvements – Strip monopole

## Microstrip – fed Strip monopole

Rogers RO5880 substrate ($\varepsilon_r$ = 2.2)
Thickness = 1.6 mm,
Length = 40 mm.,
Width = 30 mm.

Impedance Match

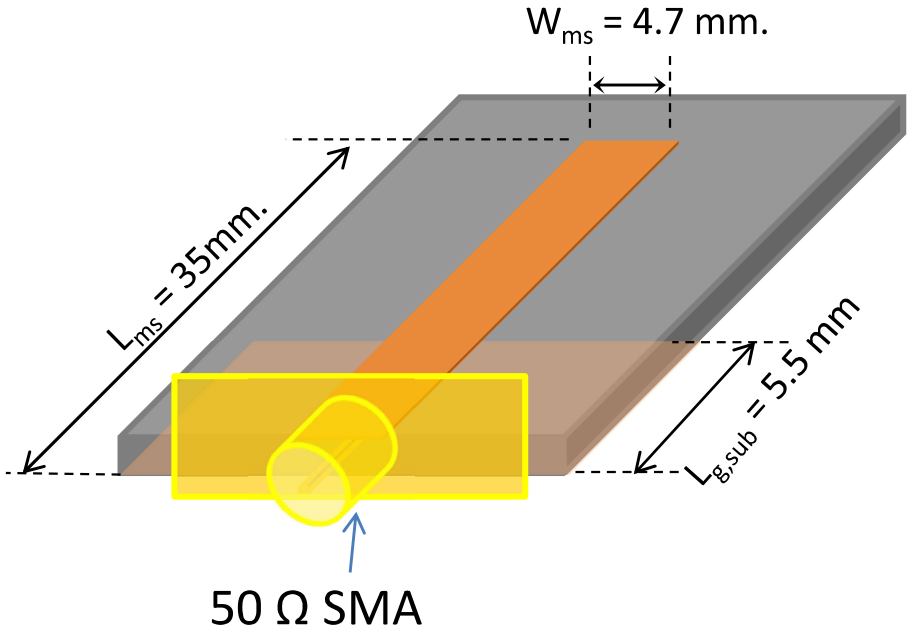


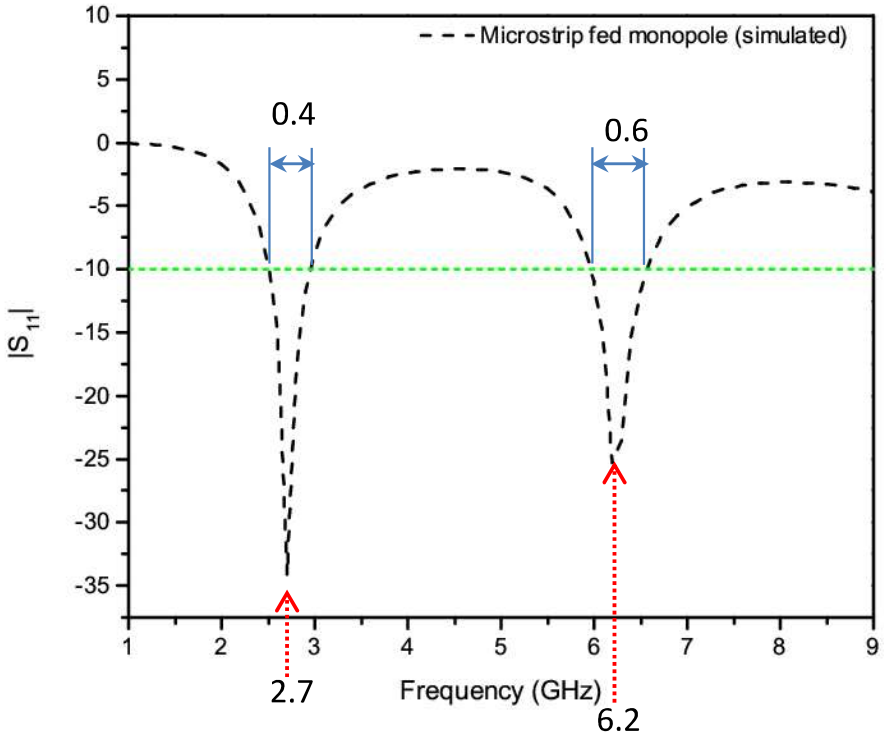

# 5.2 Design improvements – Strip monopole

## Microstrip – fed Superstrate loaded Strip monopole

Superstrate of Substrate dimensions added on top

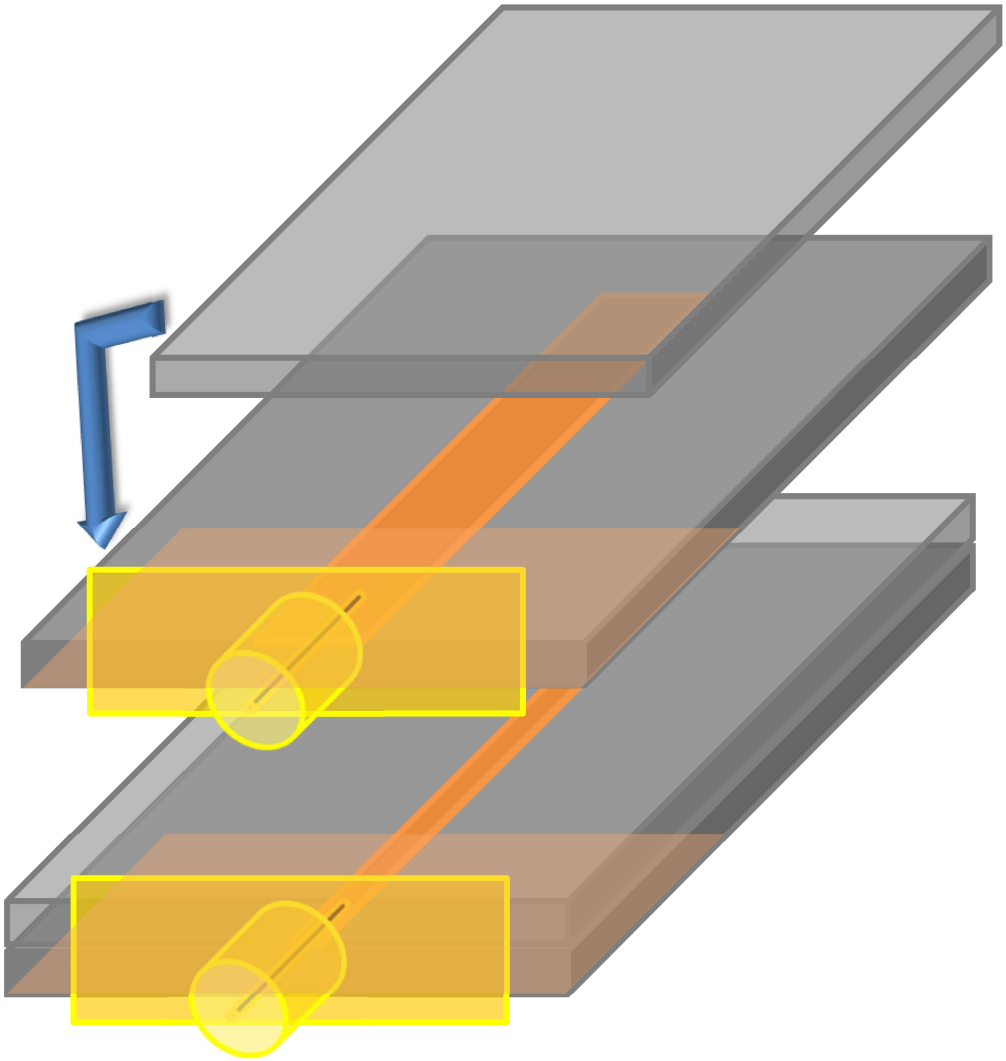

Impedance Match

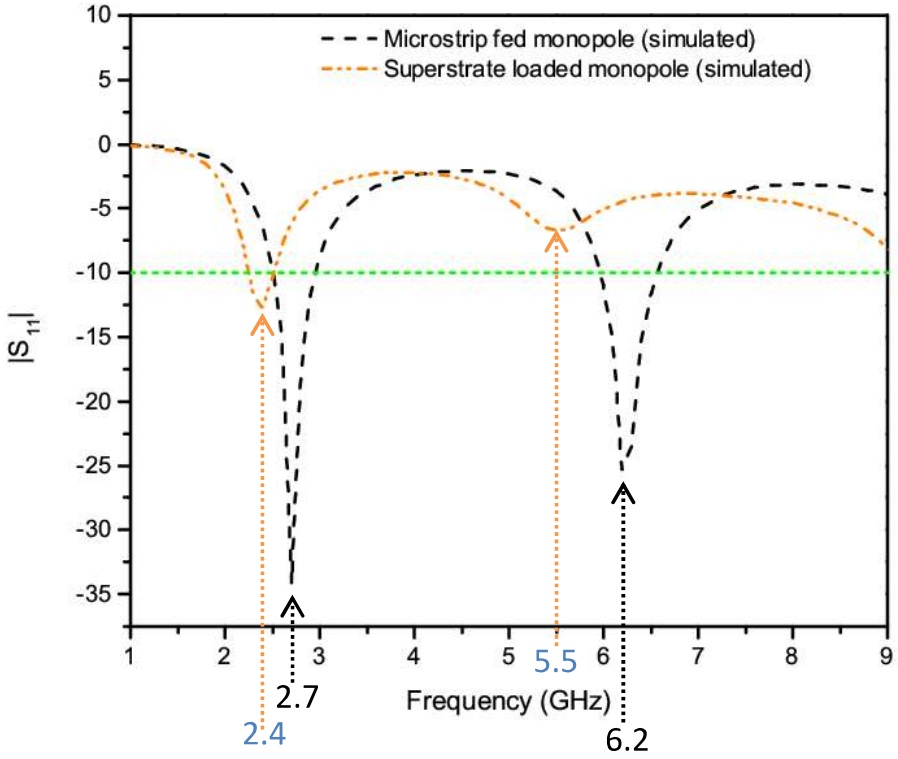


Decrease in resonant frequencies

# 5.2 Design improvements – Strip monopole

## Stripline – fed Superstrate loaded Strip monopole

Ground plane added on top of Superstrate board.

Ground plane dimensions same: [illegible] mm.

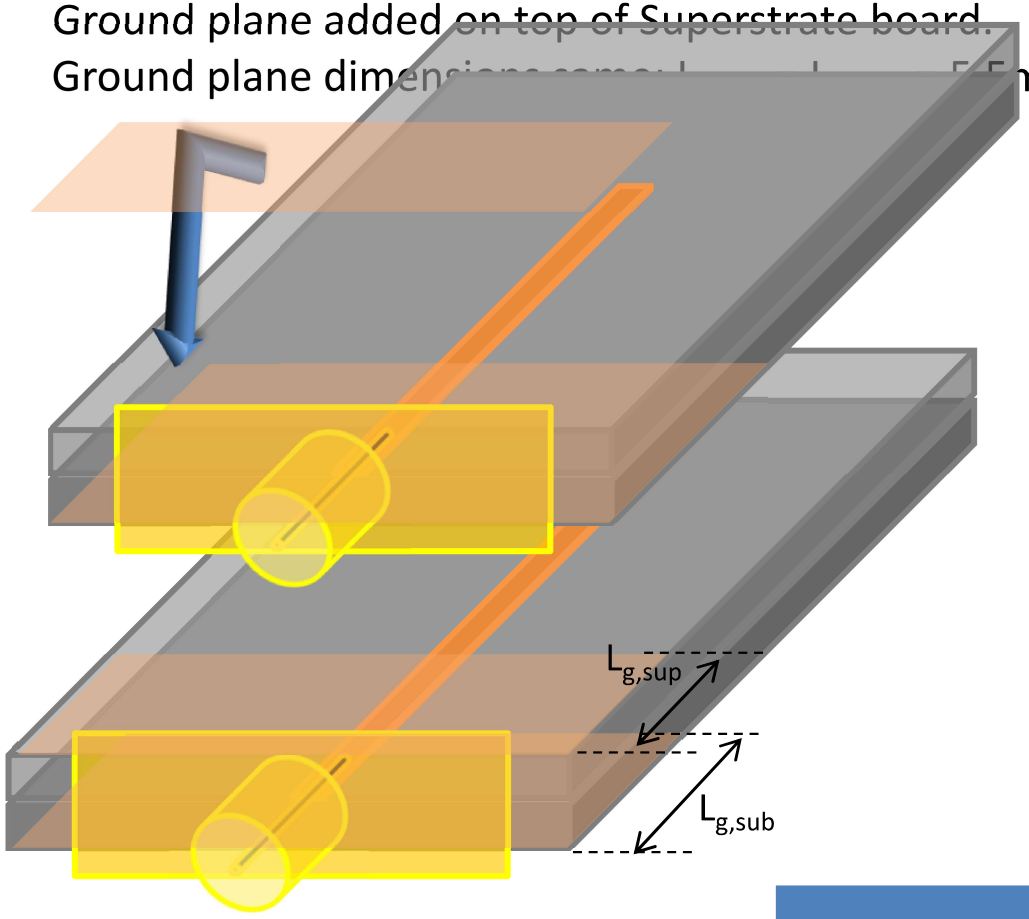


## Impedance Match

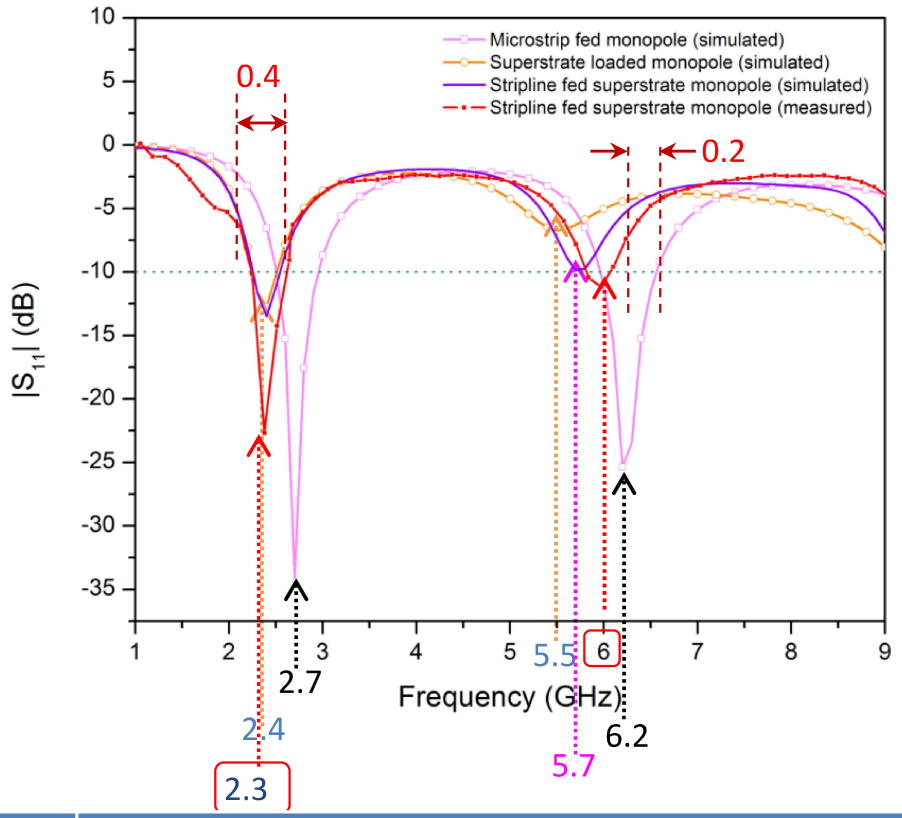


- ✓ Better resonance depth as compared to bare superstrate
- ✓ Wide bandwidth – enough for WiMAX/ WLAN operation

| Resonance Type | Frequency Reduction (with respect to Microstrip-fed strip monopole) | |
|---|---|---|
| | Simulated | Measured |
| Dominant ( 1st) | 11.1 % | 14.8 % |
| Secondary (2nd) | 8 % | 3 % |

# 5.2 Design improvements – Strip monopole

E – Plane

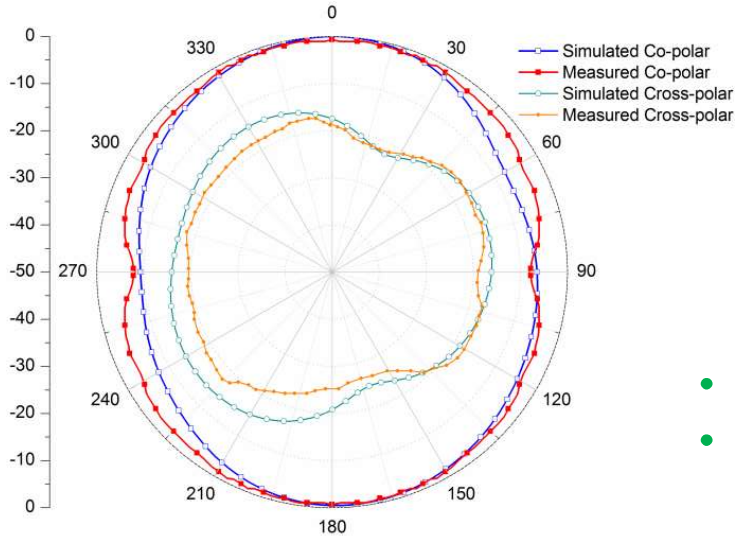


Microstrip – fed @2.7 GHz

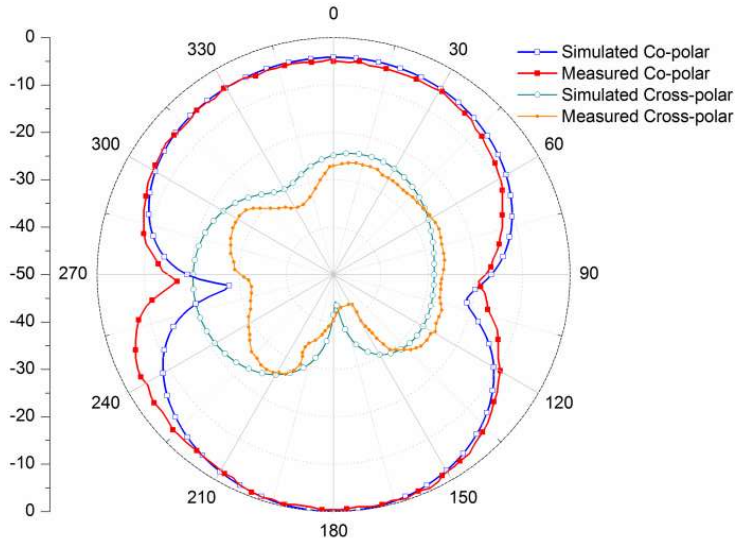


Stripline – fed @2.4 GHz

- Stripline-fed Superstrate Topology shows about 40% improvement (5.8 dB) improvement in cross polar discrimination:

  Cross-polar levels: :
  20.23 dB (stripline-fed superstrate) Vs
  14.42 dB (microstrip- fed)

- Dipole type radiation pattern
- H-plane radiation patterns do not show much improvement in cross-polar levels

(a)

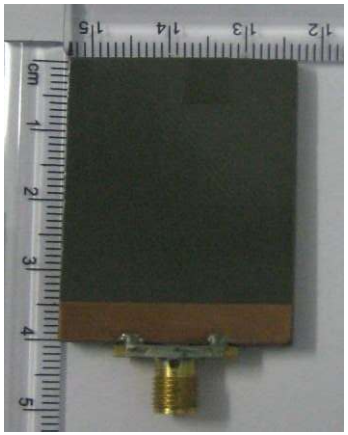

(b)

(a) Microstrip-fed strip monopole and (b) Sandwich strip monopole – Fabricated antennas

## 5.2 Design improvements – Strip monopole

### Effect of Shape modification of Ground Planes

- Triangles added symmetrically about the strip monopole axis.
- Triangles added on either of or both ground planes

{ Isosceles Triangles
$h_{tr}$ = 4.5 mm, $w_{tr}$ = 9 mm

Observation

Incremental shift of about 100 MHz/triangle pair in Secondary Resonance,
2 triangles (one face): 100 MHz & 4 triangles (both faces): 200 MHz w.r.t. 5.7 GHz
No change in dominant resonance frequency

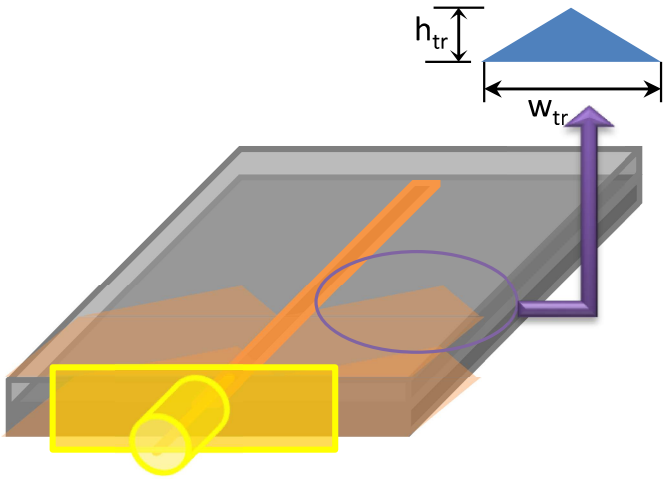


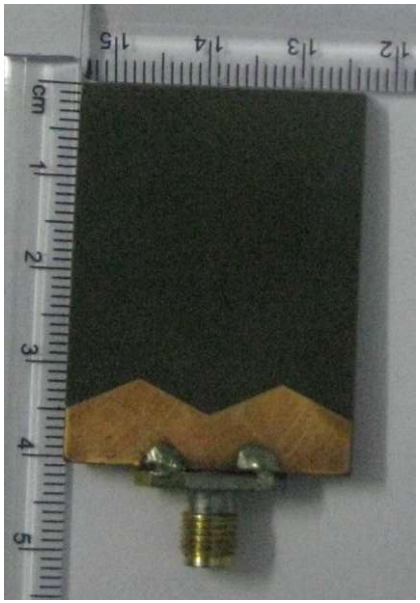

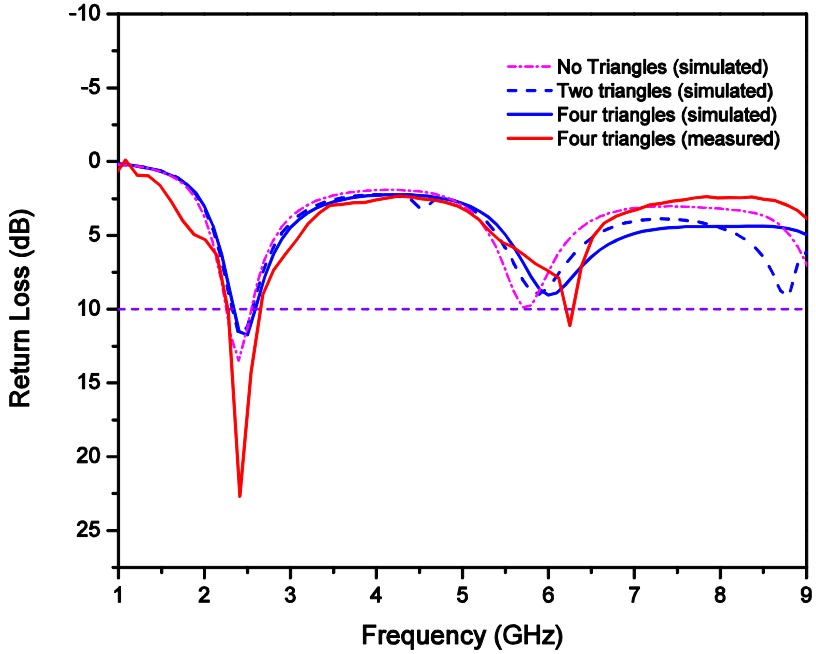

## 5.3 Adaptation of existing wideband antenna design to proposed topology

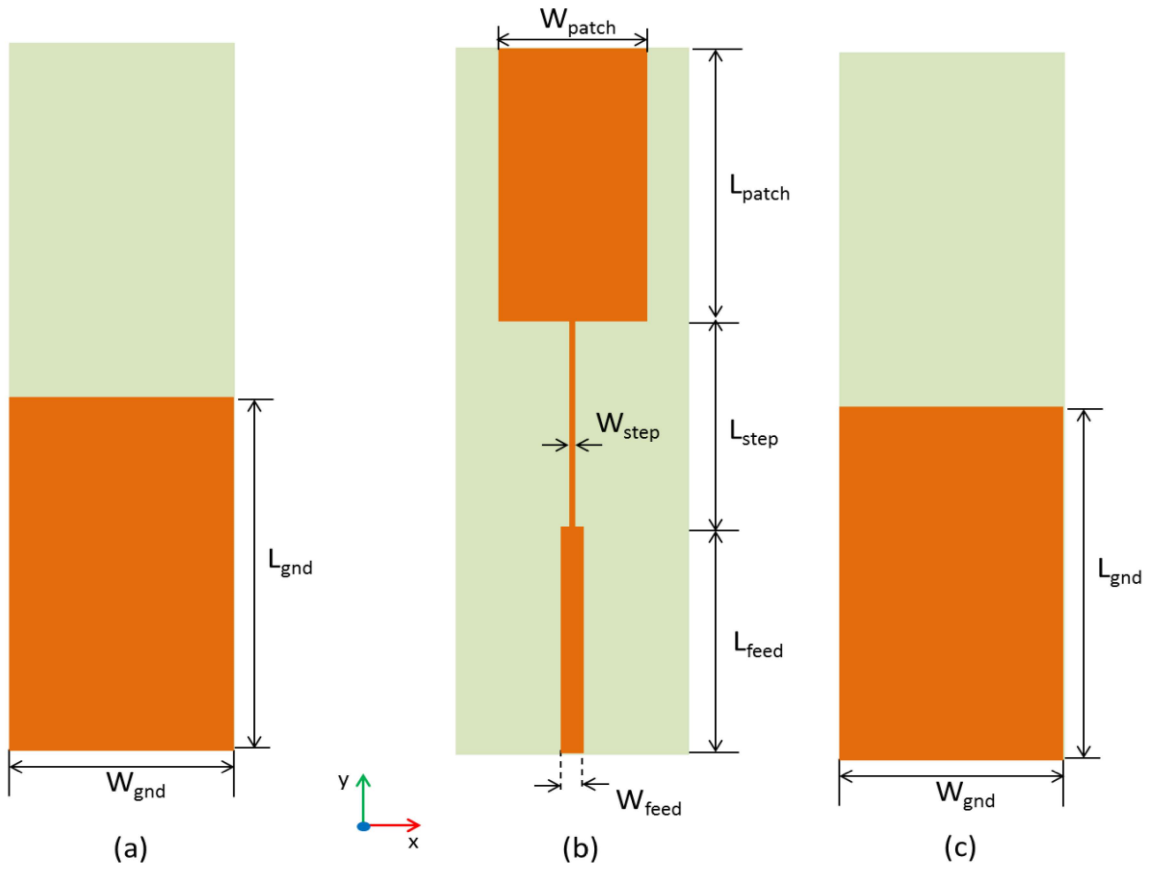


(a) Top View (b) Central 'hidden' layer and (c) Rear view schematic of wideband LTE antenna, obtained by 37% width-wise downscaling of original antenna dimensions

| Parameter | $L_{feed}$ | $L_{gnd}$ | $L_{patch}$ | $L_{step}$ | $W_{feed}$ | $W_{gnd}$ | $W_{step}$ | $W_{patch}$ |
|---|---|---|---|---|---|---|---|---|
| Values (mm) | 30 | 50 | 45 | 30 | 1.5 | 25 | 0.75 | 15 |
| Normalized to $\lambda_g$ | 0.22 | 0.37 | 0.33 | 0.22 | 0.011 | 0.18 | 0.006 | 0.01 |

# 5.3 Adapted design – Parametric Simulations

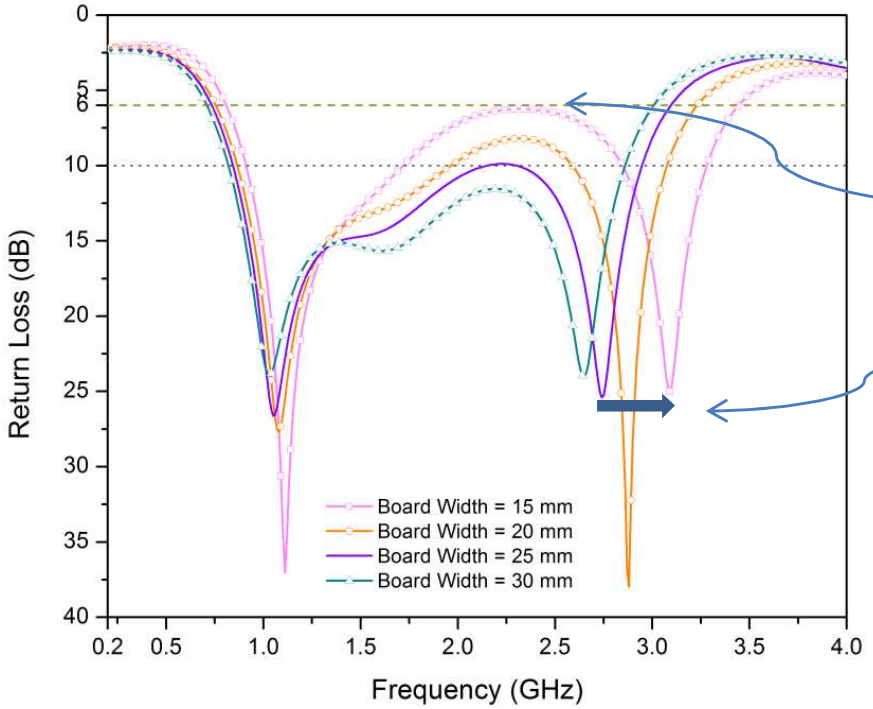


## Board width variation

Increased reflection with narrower board width

Increase in second resonance frequency with narrower board widths

## Radiator Disc width variation

Increased reflection with narrower disc width

Increase in second resonance frequency with narrower disc widths

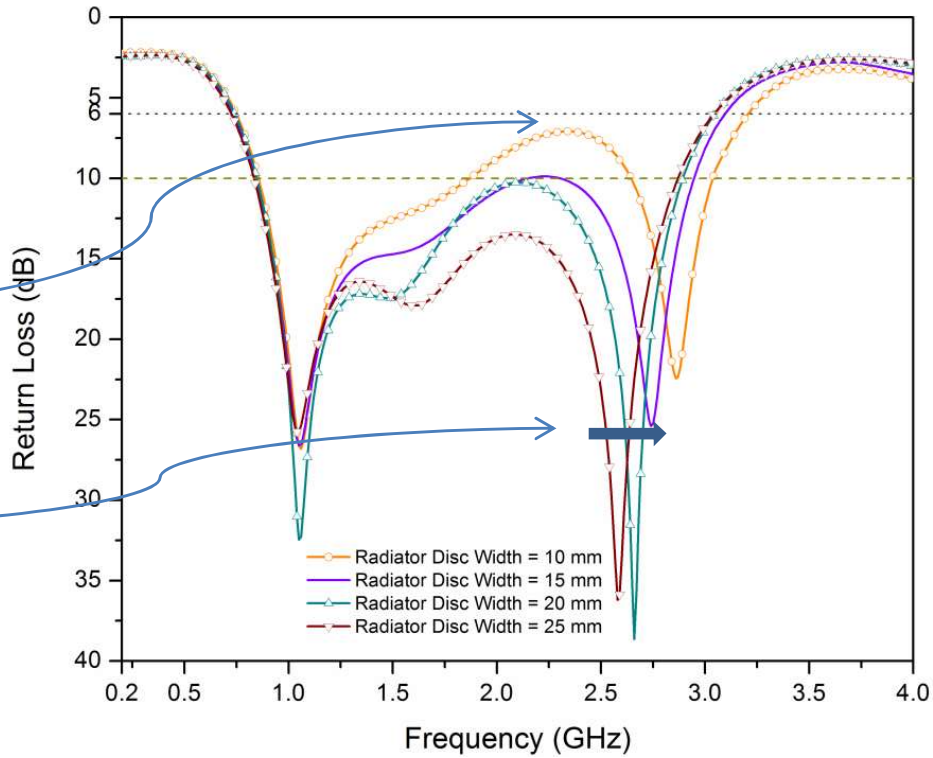

# 5.3 Adapted design – Measurements

## Return Loss measurements

Measured return loss indicate similarity in trend but also show an overall gradual shift of impedance match characteristics towards higher frequencies.

Measured results depict a range of 0.84 – 2.95 GHz (2.11 GHz, or 111.35% fractional bandwidth).

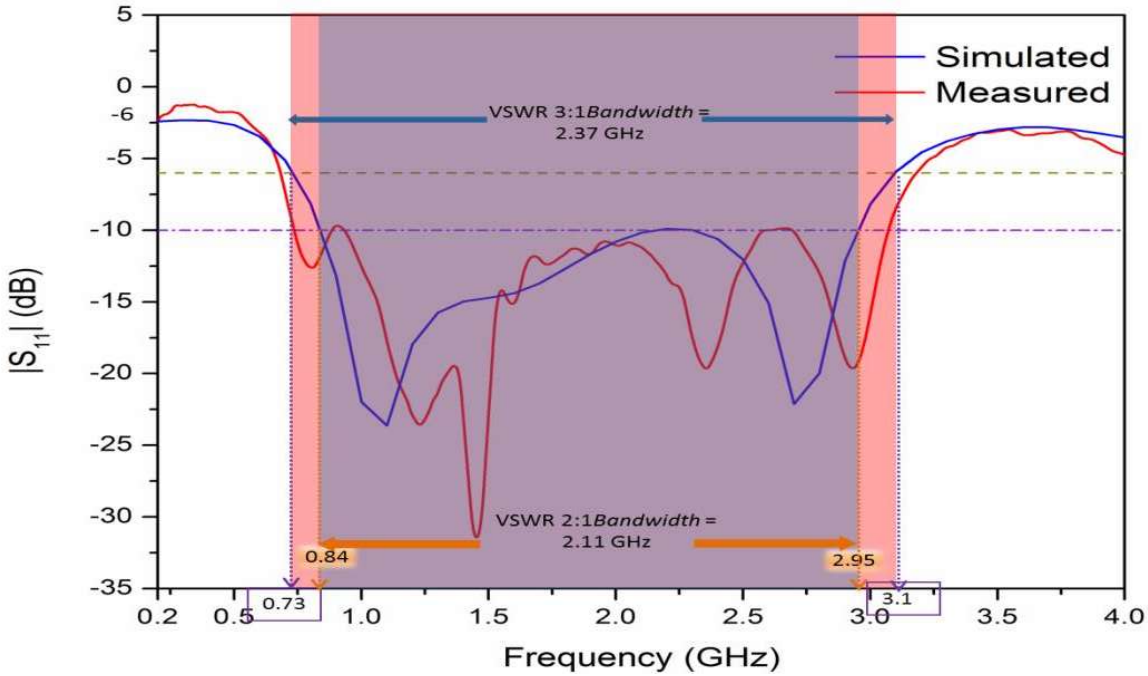


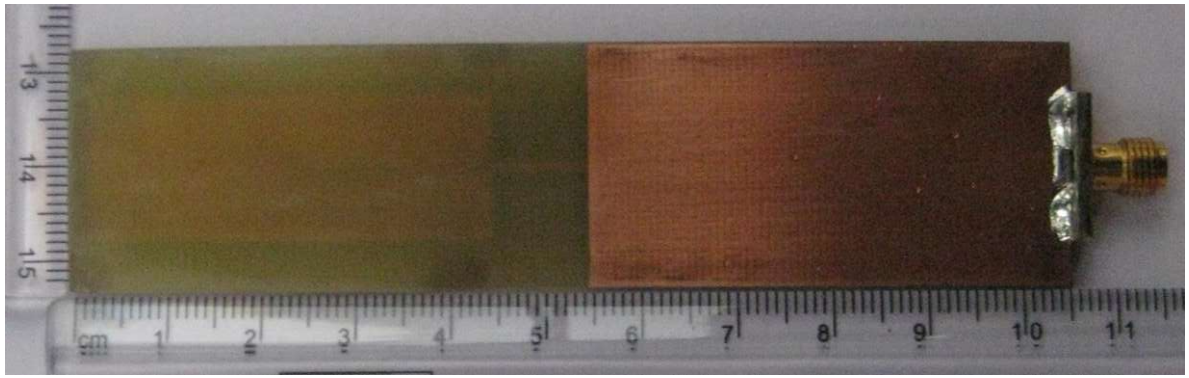

View of fabricated antenna

The sandwich wideband LTE antenna prototype is fabricated fabricated on 1/16” (1.5875 mm) thick FR4 boards ($\varepsilon_r$ = 4.4) of dimensions 105 × 30 mm$^2$.

Design dimensions are as illustrated earlier in Table 1.

# 5.3 Adapted design – Measurements

E- plane

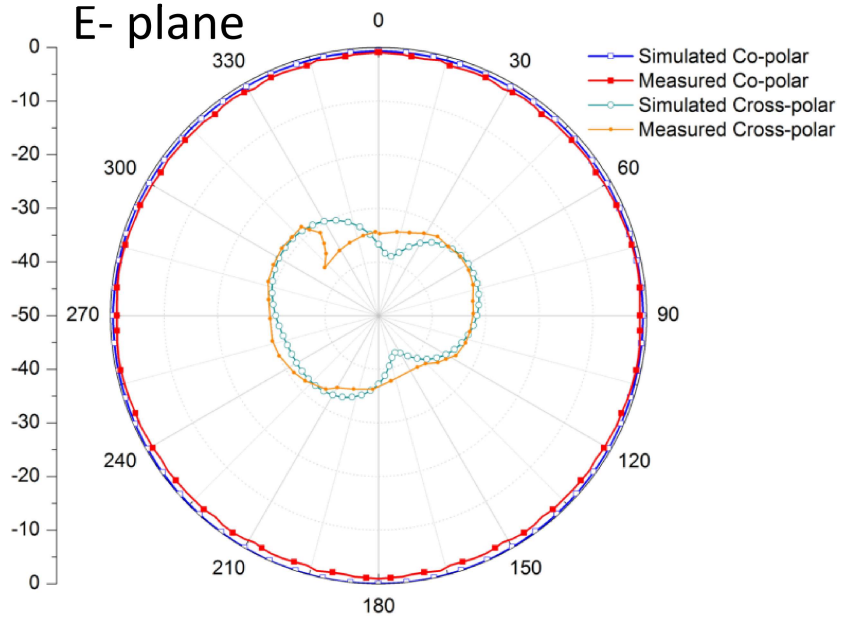


H- plane

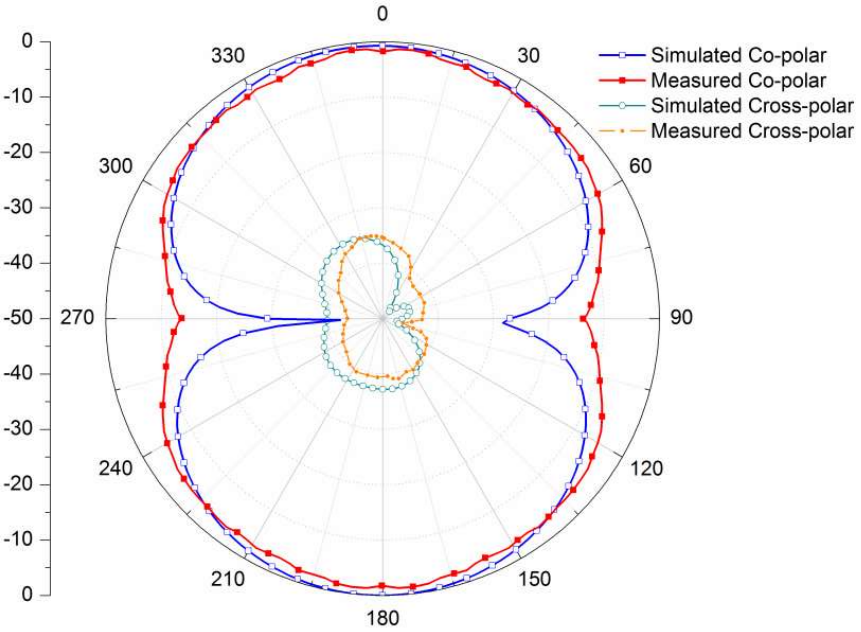


## Radiation Pattern at lowest resonant frequency (1.05 GHz)

Omnidirectional pattern with Beamwidth of 80° with radiation in broadside direction for E-plane pattern

Highly reduced cross-polar levels. Cross-polar discrimination: 34.02 dB (E-plane), and 29.1 dB (H-plane): by virtue of long-board configuration

Uni-directional longitudinal currents along feed

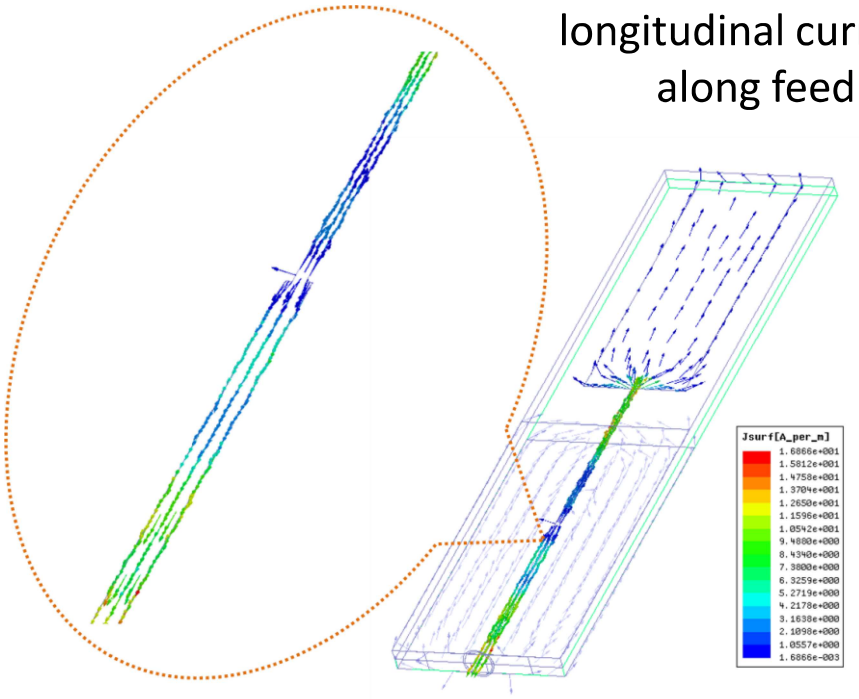

# 5.3 Adapted design – Measurements

E- plane

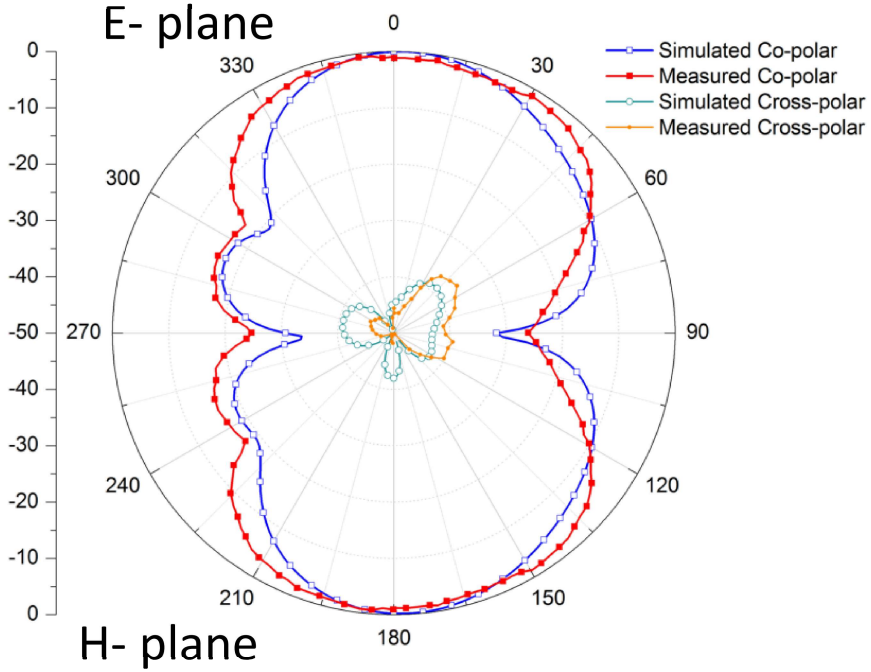


H- plane

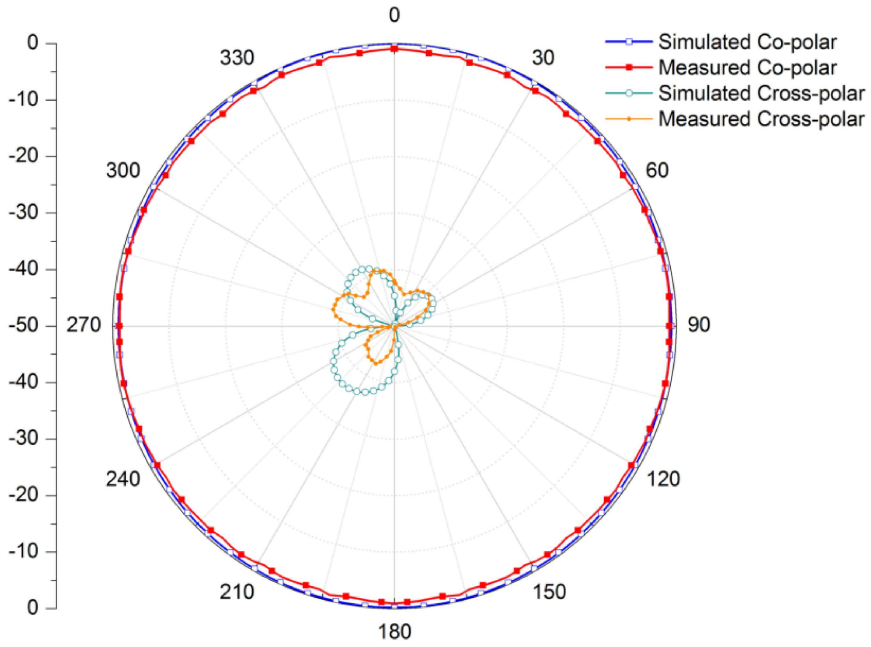


## Radiation Pattern at upper resonant frequency (2.74 GHz)

Omnidirectional pattern with Beamwidth of 60° with radiation in broadside direction for E-plane pattern; Increase in sidelobes seen due to higher order modes

Highly reduced cross-polar levels. Cross-polar discrimination: 39.02 dB (E-plane), and 35.3 dB (H-plane)

Reversal of currents along feed and on radiator

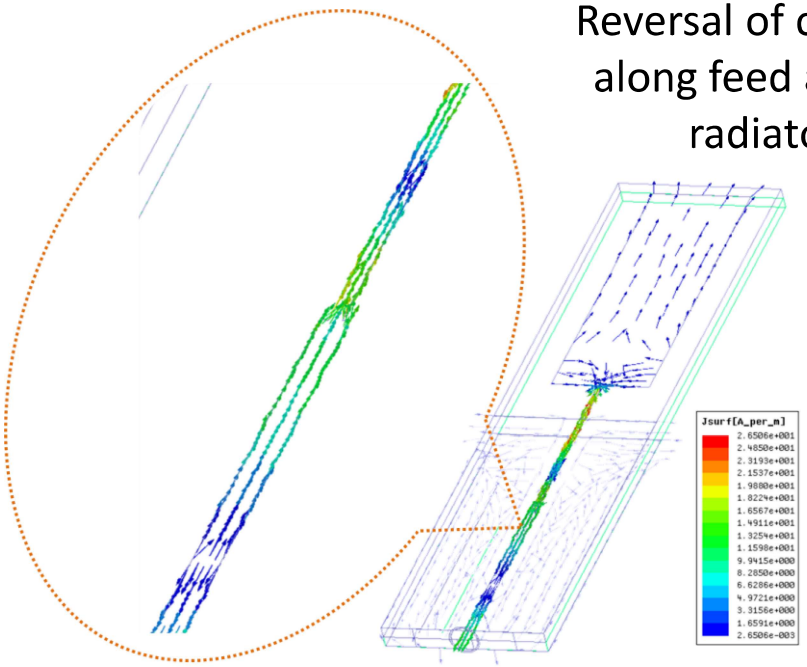

# 5.3 Adapted design – Measurements

## Gain

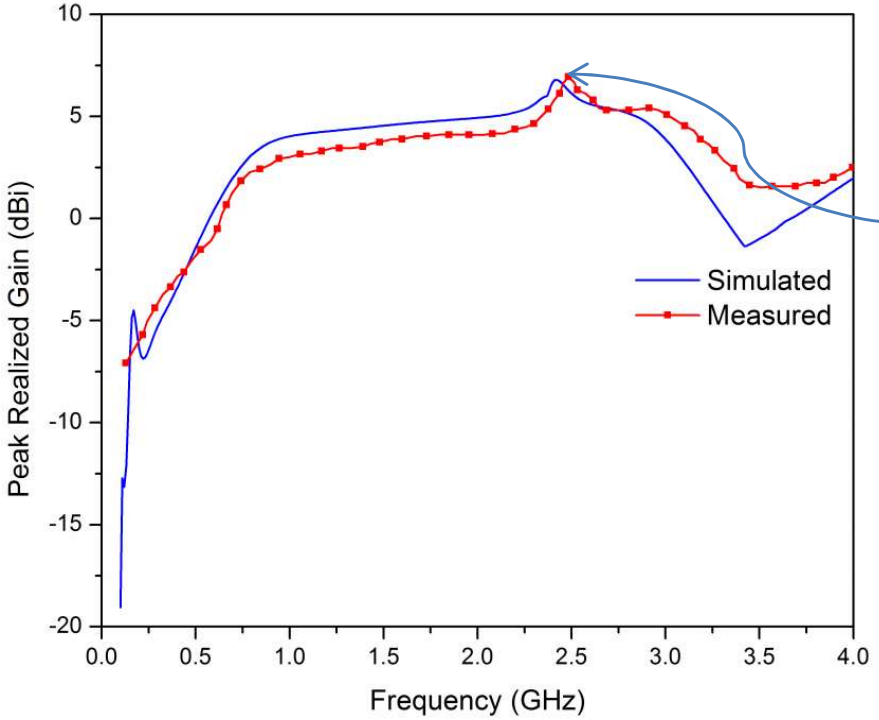


Gain lies within 6.7 dBi and shows a gradual increasing trend.

Peak Gain of 6.7 dBi around 2.4 GHz (close to second resonance frequency)

Gain starts to taper off at higher frequency due to poor impedance match

## Radiation Efficiency

Peak efficiency of 96.5 % at 0.73 GHz, and a gradual decrease to 63.2% around 3.1 GHz.

An intermediary spike of 85% is seen near the second resonance frequency.

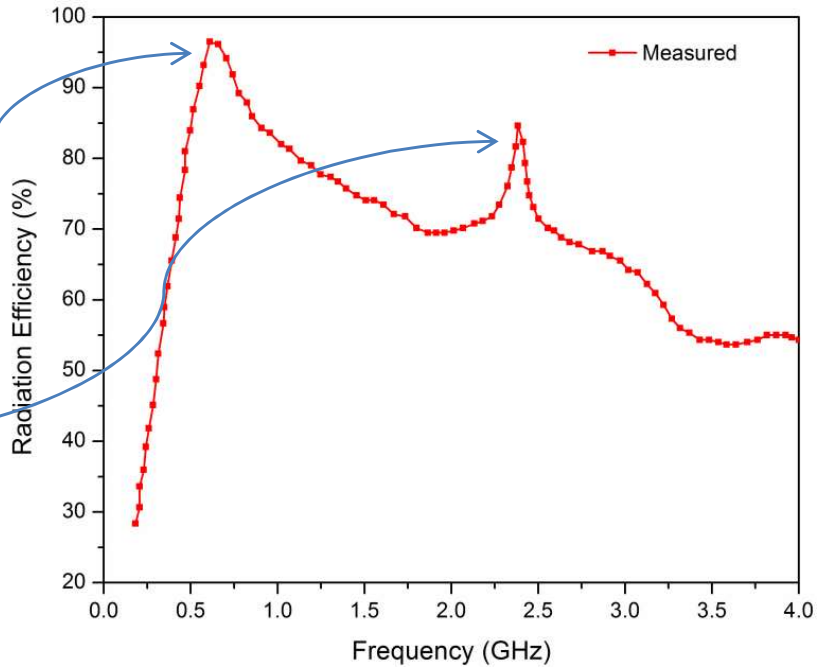

## 5.4 Summary

- A significant downward shift of dominant resonance frequencies (up to 11 %) of a narrowband strip monopole implemented in the proposed topology, as compared to its microstrip-fed counterpart.

- A comparative 3-fold increase in E-plane gain is also observed and the radiation pattern becomes more directive in the boresight direction.

- Current redistribution across two ground planes is seen to lower the cross-polarization component of the strip monopole antenna.

- Fine tuning capabilities of an extra ground plane are demonstrated where quantized secondary resonance shifts are obtained based on multiplicity of structures (here, saw-tooth isosceles triangles) attached to edges of either or both ground plane sections of the strip monopole antenna.

- It has been shown possible to miniaturize an existing wideband microstrip-fed antenna by scaling down size of the given antenna along a particular dimension without any significant modification to its shape. This width-wise dimensional downscaling, achieved with 37.5 % area reduction still finds the structure retaining its impedance match and radiation characteristics nearly as before.

# 6. Contribution of the Thesis

Demonstrating higher levels of optimization in antenna miniaturization through **shape modifications** alone and reach very low resonance frequencies despite using a lesser permittivity substrate.

Demonstrating improved miniaturization with better **structural adaptations** of simple, regular shaped geometrical dimensions but with appropriate sizing. Utility of long-board configuration in improving cross-polar discrimination is seen.

Towards development of a more **structured approach**, and less complex mathematical model for wideband antenna designs with a simple geometry – potential for fast prototyping.

**Topology modification** for improvements in miniaturization and radiation performance by proposing a stripline-fed superstrate monopole topology and demonstrating its effective utility in dimensionally downscaling an existing wideband antenna while retaining its impedance match and radiation performance.

Demonstrating the all-round contribution of ground plane re-shaping (curved ground), sizing (ground plane length for feed gap) and re-structuring (twin-tuning stubs and double ground plane) to achieve the aforementioned objectives.

# 7. Novelty of the work

- Design of an antenna with the smallest possible area footprint of 48 × 44 $mm^2$ for achieving a very low narrowband frequency match at 630 MHz, besides offering wideband and band-reject functionalities over a significant segment of the LTE domain.

- Design of an ultrawideband antenna in the LTE spectrum providing coverage over nearly *all* FDD and TDD LTE bands, while maintaining good cross-polar discrimination and omnidirectional pattern with high radiation efficiency over the entire bandwidth and with a antenna footprint (105 × 40 $mm^2$)

- Generation of a 'double-step' shaped dual-resonant high frequency wideband antenna of 35 × 30 $mm^2$ dimensions, following application of a systematic design approach harnessing miniaturization potential of stepped impedance resonator theory. Also, fine tuning in between antennas' resonances by ground plane based stubs is demonstrated to render the compact antenna operational over an ultra-wide bandwidth (3.2 – 11 GHz), which coincides nearly with the entire FCC UWB spectrum.

- Development of the 'stripline-fed superstrate' topology, and demonstrating significant shift downwards in dominant resonance and improvement in cross-polar levels of strip monopoles compared to their microstrip-fed counterparts.

- Further, achieving width-wise direct downscaling of the previously discussed low frequency rectangular disc wideband antenna to this topology with retention of its original wideband and radiation characteristics, but with a 37.5 % reduction in surface area.

# 8. Conclusion

- The research extends scope of various aspects of miniaturization in achieving lower frequencies of operation or wider operational bandwidths with lesser antenna area: shape alteration, structural optimization, theoretical modeling and topology adaptation.

- Despite inverse relationship of the guide wavelength with permittivity, lower permittivity substrates have been used to develop antennas and even for low frequency operation, have still been found to demonstrate better miniaturization and radiation efficiencies than most of their higher dielectric counterparts.

- Physical size reduction of antenna by dimensional downscaling was demonstrated.

- Ground plane significance through its relevant shaping (curved), sizing, perturbing (stubs) and re-structuring (topology) in miniaturization was highlighted.

- The research inspires use of conservative design improvement practices with cross-combining aspects of miniaturization to attain better solutions.

# 9. Scope of future work

- A further scope of improvement for the annular split ring multiband antenna lies in reducing the width of band-rejection characteristics at shorter sleeve lengths. Also, methods to decrease high cross-polarization levels observed in the above antenna can be investigated while keeping the overall antenna dimensions small.

- For the rectangular disc wideband antenna, an area of improvement can be in reducing its length dimension and relaxing restrictions on its width requirements, but while maintaining or improving its wideband impedance match characteristics. Also, the cross-polar discrimination levels should be kept within a pre-defined range during this process.

- An investigation into asymmetric ground planes in the ‘sandwich’ topology can be carried out to ascertain its miniaturization effects.

- Theoretical calculations of the radiation efficiency based on practical dielectric and metal loss data of the materials used in the prototypes can be performed and compared to the measurement data with a scope of developing relevant theoretical models for planar monopole antennas.

# References


Image references:

[a] Image source: http://sss-mag.com/spectrum.html

[b] Image source: http://www.intechopen.com/source/html/37715/media/image1.png

[c] Image source: http://www.offthereservation.net/2013/04/aereo-future-of-television.html

[d] Image source: https://www.cst.com/Content/Articles/article271/Monopole%20Antenna%20with%20Notch%20Filter%20Components.gif

[e] Image source: http://www.nanotech-now.com/news_images/42004.jpg

Text References:

[1] C.-L. Hu, D.-L.Huang, H.-L.Kuo and C.-F.Yang, "Compact multibranch inverted-F antenna to be embedded in a laptop computer for LTE/WWAN/IMT-E applications", *IEEE Antennas Wireless Propag.Lett.,*vol. 9, pp. 838-841, 2010

[2] K.-L Wong and T.-W. Weng, "Small-size triple wideband LTE/WWAN tablet device antenna", *IEEE Antennas Wireless Propag.Lett.,*vol. 12, pp. 1516-1519, 2013.

[3] W. Zhou and T. Arslan, "Planar monopole antenna with Archimedean spiral slot for WiFi/Bluetooth and LTE Applications", in *Proc. Loughborough Antennas Propag. Conf. (LAPC)*, Loughborough, UK, pp. 186-189, 2013.

[4] S. Ahmed, F. A. Tahir, A. Shamim and H. M. Cheema, "A compact Kapton-based inkjet printed multiband antenna for flexible wireless devices", *IEEE Antennas Wireless Propag. Lett*., vol. 14, issue.c, pp. 1802-1805, 2015

[5]Y.-L Ban, C.-L. Liu, J. L.-W. Li and R. Li, "Small-size wideband monopole with distributed inductive strip for seven-band WWAN/LTE mobile phone", *IEEE Antennas Wireless Propag.Lett.,*vol. 12, pp. 7-10, 2013.

[6] B. Sanz-izquierdo and R. Leelaratne, "Evaluation of Wideband LTE Antenna Configurations for Vehicle Applications," in *Proc. Loughborough Antennas Propag. Conf. (LAPC)*, Loughborough, UK, pp. 383-387, 2013.

[7] W.-S. C. W.-S. Chen, Y.-T. C. Y.-T. Chen, H.-T. C. H.-T. Chen, and J.-S. K. J.-S. Kuo, "Wideband printed monopole antenna for wireless applications," *2009 IEEE Antennas Propag. Soc. Int. Symp.*, no. l, pp. 3–6, 2009.

[8] J. Liu, K. P. Esselle, S. G. Hay, and S. Zhong, "Achieving ratio bandwidth of 25:1 from a printed antenna using a tapered semi-ring feed," *IEEE Antennas Wirel. Propag. Lett.*, vol. 10, pp. 1333–1336, 2011.

[9] Z. Guo, H. Tian, X. Wang, Q. Luo, and Y. Ji, "Bandwidth enhancement of monopole uwb antenna with new slots and ebg structures," *IEEE Antennas Wirel. Propag. Lett.*, vol. 12, pp. 1550–1553, 2013.

[10] S. L. Zuo, Z. Y. Zhang, and J. W. Yang, "Planar meander monopole antenna with parasitic strips and sleeve feed for DVB-H/LTE/GSM850/900 Operation in the mobile phone," *IEEE Antennas Wirel. Propag. Lett.*, vol. 12, pp. 27–30, 2013.

[11] M. Rabah, D. Seetharamdoo, R. Addaci, and M. Berbineau, "Novel miniature extremely-wide-band antenna with stable radiation pattern for spectrum sensing applications," *IEEE Antennas Wirel. Propag. Lett.*, vol. 1225, no. c, pp. 1–1, 2015.

[12] Kin-Lu Wong, Yin-Fang Lin, "Stripline-fed printed triangular monopole", Elect. Letters, Vol. 33, Issue 17, pp. 1428 – 1429 , Aug. 1997